

THE ADEQUACY OF STELLAR EVOLUTION MODELS FOR THE INTERPRETATION OF THE COLOR-MAGNITUDE DIAGRAMS OF RESOLVED STELLAR POPULATIONS

C. Gallart

Instituto de Astrofísica de Canarias, Tenerife, Canary Islands, Spain;
email: carme@iac.es

M. Zoccali

Department of Astronomy and Astrophysics, Pontificia Universidad Católica de Chile,
Casilla 306, Santiago 22, Chile; email: mzoccali@astro.puc.cl

A. Aparicio

Instituto de Astrofísica de Canarias, 38200 La Laguna, Tenerife, Canary Islands,
Spain; email: antapaj@iac.es

Key Words AGB stars, horizontal branch, main sequence, red giant branch, stellar content

■ **Abstract** Most of what we know about the stellar population of nearby, resolved galaxies comes from the interpretation of their color-magnitude diagrams, by comparison with stellar evolutionary models. We review how well current stellar evolution models reproduce the properties of simple stellar populations. Emphasis is given to the regions of the color-magnitude diagram which are most useful for deriving age, metallicity, or distance of a population. Extensive comparison is made between the predictions of the most-used stellar evolution libraries, in order to estimate how model dependent the results are.

The present review, written from a user perspective, aims at emphasizing the strengths and weaknesses of the models, and is intended both for observers and theoreticians. We hope to encourage observers to provide stronger observational constraints where they are needed, and to stimulate theoreticians to isolate the input physics responsible for the different behavior between models and the reasons for the discrepancies with data.

1. INTRODUCTION

In the last few years, there has been a growing interest in the determination of the star formation history (SFH) of nearby, resolved galaxies. The discovery of

multiple stellar populations in most Milky Way dSph satellite galaxies and the new opportunities offered by the HST to extend these studies to a variety of environments and galaxy types over the whole Local Group and beyond have been key developments fueling renewed interest in the subject. The interpretation of the color-magnitude diagrams (CMDs) of composite stellar populations, however, relies heavily on stellar evolution models, and their strengths and weaknesses directly affect the reliability of the conclusions of any CMD analysis. Stellar evolution models oriented to the study of stellar populations in galaxies need to reliably include a wide range of ages and metallicities. Their testing needs to go beyond the classical tests using Milky Way clusters as templates; the templates should include clusters in other galaxies, such as the Magellanic Clouds, where there are populous clusters of all ages and metal enrichment patterns different to those in the Milky Way. In some cases, especially when dealing with very short stellar evolutionary phases (e.g., the asymptotic giant branch, AGB), the CMDs of nearby galaxies may also be used as calibrators.

In this review, we discuss the common methods used to retrieve information on the SFH from various sequences in a complex CMD, and how the results are affected by current stellar evolution uncertainties. We critically review the current status of stellar evolution modeling, with emphasis on those evolutionary phases most relevant for SFH determinations. In this context, a review of the main observational tests of stellar evolution models is presented. Emphasis is given to intermediate- and low-mass stars, because high-mass stars represent only a very small percent of the whole SFH in a galaxy. Previous *ARAA* papers have discussed the topic of massive star evolution and populations (Chiosi & Maeder 1986, Maeder & Conti 1994, Massey 2003).

In the interpretation of composite CMDs, sets of stellar models are usually taken as black boxes. Often one set is preferred over another for the extension (or finer step) of the grid in metallicity or age. One way to estimate the current global uncertainties of stellar evolution models is to compare the predictions of various sets, at face value. Here we do this systematically for all evolutionary phases discussed. Whenever possible, observational data is added to the comparison. We highlight the impact that the differences among models may have in the derived SFHs. Owing to space limitations, we do not discuss other sources of uncertainty in deriving SFHs, such as observational errors, the presence of binary stars, uncertain or variable reddening, and differences among metallicity scales. On the other hand, we do not aim to summarize our knowledge of stellar evolution or the SFHs of nearby galaxies. Classic review papers by Iben & Renzini (1983), Renzini & Fusi Pecci (1988), Iben (1991) and Chiosi, Bertelli & Bressan (1992) cover the first topic, and Sandage (1986), Hodge (1989), Olszewski, Suntzeff & Mateo (1996), Mateo (1998) discuss the second. Finally, we do not discuss the valuable information on the SFH provided by variable stars, and we mainly restrict ourselves to the most widely used *V* and *I* optical bands.

This review is organized as follows: In Section 2, we summarize the characteristics of the stellar evolution libraries that are discussed in the rest of the review. In Section 3, we present the current methods used to derive SFHs from deep

CMDs. In the remaining sections, we discuss each main stellar evolution phase, namely the main sequence (MS), the red giant branch (RGB), the horizontal branch and red clump (HB, RC), and the AGB (provided as Supplemental Material; follow the Supplemental Material link from the Annual Reviews home page at <http://www.annualreviews.org/>). In each case, we provide (a) a brief description of the physical processes that occur in the star; (b) a discussion of the information on the SFH provided by that phase, and a review of the ways in which it has been used; (c) a comparison of the predictions of a number of stellar evolution libraries; and (d) a discussion of the main uncertainties that affect the modeling of that phase and the related observational tests. We conclude with a summary of the main issues that need to be taken into account regarding each stellar evolution phase when using stellar evolution models to derive properties of resolved stellar populations and a few remarks on the expected progress in the field.

2. STELLAR EVOLUTION LIBRARIES

We will preferentially discuss the most current stellar evolution libraries that provide a wide coverage of the age–metallicity parameter space and that are therefore most useful for the study of the CMDs of galaxies. These include some that have already been heavily used and other very recent ones that are likely to be used in the future. We will only occasionally discuss (if at all) libraries that refer to a limited range of masses and/or metallicities (e.g., Stothers & Chin 1991; Jimenez & McDonald 1996; Baraffe et al. 1998; Ventura et al. 1998; Bono et al. 2000; Montalbán, D’Antona & Mazzitelli 2000; Claret 2004).

Table 1 presents a summary of the characteristics of the selected stellar evolution libraries. The first five lines describe the parameter space covered by the models: the mass and metallicity range, whether they include calculations with α -enhanced mixtures of heavy elements or are restricted to scaled solar composition, and details of the transformation to the observational plane. The remaining lines refer to the main model input physics. The first group refers to the *microphysics*, including atomic and nuclear properties such as equation of state, nuclear reaction rates, opacity, or neutrino energy losses. The second refers to the main parameterizations adopted: solar calibration, He-enrichment ratio, mixing length (α_{MLT}), and occurrence or absence of diffusion and overshooting. [*]

It is difficult, from a user point of view, to isolate which ingredients produce particular differences among libraries. In each one, some of the parameterizations may be fine-tuned (e.g., mixing length) to reproduce the observational constraints with the adopted physics, and in general models indeed reproduce observations fairly well. No estimate is given in general of models’ uncertainties introduced, for example, by varying the input physics within a reasonable range (praiseworthy exceptions are Stothers & Chin 1993, Chaboyer & Kim 1995, Cassisi et al. 1998, Castellani et al. 2000, Chaboyer & Krauss 2002). In this paper, we mainly discuss the parameterizations of stellar evolution models that particularly affect

TABLE 1 Physical inputs and assumptions adopted in the selected stellar evolution libraries

Models	Teramo	Girardi	Bertelli	Geneva	YY	Victoria	Pisa	Pols	Straniero
Mass range (M_{\odot})	0.5–10	0.15–7	0.6–120	0.8–120	0.4–5.2	0.5–1.3	0.6–11	0.5–50	0.6–25
Z range (nstep)	0.0001– 0.04 (10)	0.0–0.07 (10)	0.0004–0.05 (5)	0.0004–0.1 (7)	0.00001– 0.08 (11)	0.0001– 0.01 (17)	0.0002– 0.008 (6)	0.0001–0.03 (7)	0.0001–0.02 (7)
Z Mixture ^a	SS+ α (0.4)	SS+ α (0.4)	SS	SS	SS+ α (0.3,0.6)	SS+ α (0.3,0.6)	SS	SS	SS
Color- T_e Rel.	CK03	CGK97+AF94	K92+empirical	LCB97+LCB98	LCB98+GDK87	VC03	C99	K92	CGK97
Phot. Bands ^b	J-C-IR-HST	J-C-IR-HST-W-ESO	J-C-IR	J-C-IR-HST-G-W	J-C-IR	BVRI	J-C	J-C	J-C-IR
EOS	I04	KTW65+S88,MHD90	KTW65	CG68	EOSOPAL+CK95	updated V92	EOSOPAL+S88	P95	S88
Nucl. Reactions	NACRE+K02	CF88+L90+WW93	CF88	CF88+C85+L90	BP92	BP92	NACRE	CF88+C85	CF88+C85
Radiative	OPAL96+AF94	OPAL92+AF94	OPAL92+H77+C70	OPAL92+K91	OPAL96+AF94	OPAL92+AF94	OPAL96+AF94	OPAL92+AF94	OPAL92+AF94
Opacity									
Conductive	P99	HL69	HL69	HL69	HL69+C70	HL69	I83	—	I83
Opacity									
Neutrinos Losses	HRW94+MKI85	MKI85+IK83	MKI85	I89	I89	I96	I96+HRW94	I89+I93	MKI85

[*]

Y_{\odot}, Z_{\odot}	0.2734,0.0198	0.273,0.019	0.282,0.02	0.299,0.0188	0.267,0.0181	0.2715,0.0188	0.289,0.0198	0.2812,0.0188	0.285,0.02
$Y_p, \Delta Y/\Delta Z$	0.245,1.4	0.23,2.25	0.23,2.55	0.24,3.0	0.23, 2	0.235,2	0.23,2.5	0.24,2.0	0.23,~2.5
$\alpha_{MLT} = I/H_p$	1.913	1.68	1.63	1.6	1.74	1.89	1.9,2.3	2.0	2.2
Diffusion	no (only for Sun)	no	no	no	yes	no	yes	no	yes
Core Over: ^c λ_{OV}/H_p	0.0 & 0.20	0.50	0.50	0.20	0.20	0.0	0.0	yes	no
Env. Over: ^c λ_E/H_p	0.0	0.25	0.70	0.20	—	0.0	0.0	yes	no

Note. **References for the model libraries:** Teramo; Cassisi et al. (2004); Pietrinferni et al. (2004); Girardi et al. (2000); Salasnich et al. (2000); Girardi et al. (2002); Bertelli; Bertelli et al. (1994); Geneva; Schaller et al. (1992), the library has been largely updated along this last decade (see Lejeune & Schaerer 2001, and references therein). Yale; Yi et al. (2001), Kim et al. (2002); Yi, Kim & Demarque (2003); data refer to the revised version (May 2003) of the library; Victoria; Vandenberg et al. (2000), Bergbusch & Vandenberg (2001); Pisa; Castellani et al. (2003), Cariulo, Degl'Innocenti, Castellani (2004); Pols et al. (1998); Straniero, Chieffi & Limongi (1997), Dominguez et al. (1999), Limongi, Limongi, Straniero & Chieffi (2000). **References for the physical inputs:** AF94; Alexander & Ferguson (1994); BP92; Bahcall & Pinsonneault (1992); C70; Cox & Stewart (1970a,b); C85; Caughlan et al. (1985); C99; Castelli (1999); CF88; Caughlan & Fowler (1988); CG68; Cox & Giuli (1968); CGK97; Castelli, Gratton & Kuznetsov (1997); CK03; Castelli & Kuznetsov (2003); CK95; Chaboyer & Kim (1995); EOSOPAL; Rogers, Swenson & Iglesias (1996); F94; Fluks et al. (1994); GDK87; Green, Demarque & King (1987); H77; Huebner et al. (1997); HL69; Hubbard & Lampe (1969); HRW94; Haefl, Raffelt & Weiss (1994); K02; Kunz et al. (2002); K91,K92; Kuznetsov (1991,1992); KTW65; Kippenhahn, Thomas & Weigert (1965); I04; Irwin et al. (2004, in preparation); I83,I89,I93,I96; Itoh et al. (1983,1989,1993,1996); IK83; Itoh & Kohyama (1983); L90; Landré et al. (1990); LCB97,LCB98; Lejeune, Cuisinier & Buser (1997,1998); MHD90; Mihalas et al. (1990); MKI85; Munakata, Kohyama & Itoh (1985); NACRE; Angulo et al. (1999); OPAL92, OPAL96; Rogers & Iglesias (1992), Rogers, Swenson & Iglesias (1996); P95; Pols et al. (1995); P99; Porekhin (1999); S88; Straniero (1988); Y92; Vandenberg (1992); VC03; Vandenberg & Clem (2003); WW93; Weaver & Woosley (1993).

^aSS = Scaled-Solar mixture, $\alpha(+x) = \alpha$ -enhanced mixture [α/Fe] = x .

^bJ = Johnson bands, C = Cousins, IR = Infrared, HST = HST bands, W = Washington system, ESO = ESO system.

^cThe parameter describing the extent of overshooting across the border of the convective zone, in units of pressure scale height (H_p). This parameter as defined in the Bressan et al. (1981) formalism is not equivalent to others present in the literature (e.g. $\lambda = 0.5$ in the Padova formalism approximately corresponds to $0.25H_p$ in the formalisms used by the other groups). λ_{OV} refers to core overshooting, while λ_E refers to envelope overshooting. The prescription on how overshooting is turned off as a function of mass is different among different authors (see references and Supplemental Figure 4; follow the Supplemental Material link from the Annual Reviews home page at <http://www.annualreviews.org/>).

the different stellar evolution phases. The reader is referred to other review papers (e.g., Chiosi, Bertelli & Bressan 1992; Salaris, Cassisi & Weiss 2002) for a discussion of different microphysics inputs.

3. METHODS FOR DERIVING STAR FORMATION HISTORIES

The CMD is the best tool for retrieving the SFH of a stellar system. CMDs that reach at least the brightest part of the RGB or better, the oldest MS turnoffs, display stars born throughout the lifetime of a galaxy and are fossil records of its SFH. But deciphering the information contained therein and deriving a quantitative, accurate SFH is complicated and requires relatively sophisticated techniques.

The term SFH can include many characteristics of a stellar system and their evolution with time: star formation rate [SFR(t)], chemical enrichment [Z(t)], initial mass function (IMF), frequency and mass distribution of binary stars, etc. However, because the quantities that are expected to vary most between galaxies are SFR(t) and Z(t), the SFH is usually defined as the function $S[\text{SFR}(t), Z(t)]$. Current methods for deriving the SFH are based on relatively automatic analysis of the density of stars across the CMD and may (Aparicio, Gallart & Bertelli 1997; Dolphin 1997) or may not (Hernández, Valls-Gabaud & Gilmore 1999) involve a parameterization of the CMD. The first approach is the one most widely used and is adopted here (Gallart et al. 1999a; see also Aparicio 2002 for a review of both methods). A Monte Carlo code and a stellar evolution library are used to generate a large number of synthetic stars with ages and metallicities uniformly distributed over the full interval of the SFR(t) and Z(t). This represents a constant SFR with uniformly distributed metallicity over the metallicity range for each age. The synthetic stars are distributed in an array of “partial” models containing stars within small intervals of age and metallicity. The set of partial models can be considered an $n \times m$ -dimensional vector space, where n and m are the number of age and metallicity intervals, respectively. Each partial model is denoted by S_i , with $i = 1$ to $n \times m$.

To compare models and observations, a set of boxes is defined in the CMD. In practice, two approaches are used: uniform grids and *à la carte* (optimized) grids. A uniform grid is more objective and less dependent on human criteria. An *à la carte* grid takes advantage of our knowledge of stellar evolution and allows different samplings of well and poorly known stellar evolution phases. An array, M_i^j , containing the number of stars from partial model S_i populating box j is computed. The same operation is made in the observational CMD, producing a vector O^j containing the number of observed stars in box j . This step defines the parameterization of the CMD. With this information, the distribution of stars in the defined boxes can be calculated for any SFH as a linear combination of the M_i^j : $M^j = A \sum_i \alpha_i M_i^j$, where A is a scaling constant. The SFH best matching the distribution, O^j , of the observational CMD can be found using a merit function

such as χ^2 or, better, χ^2_ν (as in Mighell 1999), which provides the best solution and a test of its goodness. Finally, the corresponding SFH can be written as $S = A \sum_i \alpha_i S_i$.

Various groups have performed implementations of this general method, e.g., Tosi et al. (1991); Bertelli et al. (1992); Tolstoy & Saha (1996); Dolphin (1997); Dohm-Palmer et al. (1997); Hurley-Keller, Mateo & Nemeč (1998); Gallart et al. (1999a); Hernández, Valls-Gabaud, & Gilmore (1999); Holtzman et al. (1999); Olsen (1999); Harris & Zaritsky (2001); Frayn & Gilmore (2002); Ng et al. (2002); Smecker-Hane et al. (2002). A special session was held at the meeting *Observed HR Diagrams and Stellar Evolution* (Lejeune & Fernandes 2002) with the aim of comparing the results obtained by these different groups in the interpretation of high-quality CMDs of the LMC bar (Skillman & Gallart 2002). Other papers comparing results obtained with different methods are Wyder (2001) and Skillman et al. (2003). To compute synthetic CMDs we here use the tool IAC-star (Aparicio & Gallart 2004) available on the Web at <http://iac-star.iac.es>.

4. THE MAIN SEQUENCE

The MS is the locus in the CMD of core H-burning stars. With increasing mass, at the same evolutionary stage and Z , stars are more luminous and hotter. This produces the typical MS trend across the CMD, running from a hot, luminous part to a cooler, faint one. All stars achieve equilibrium H-burning reactions on the Zero Age MS (ZAMS), but while low-mass stars, $M \lesssim 1.2 M_\odot$, evolve by becoming brighter and bluer, more massive stars evolve toward brighter luminosity but lower effective temperature, except during the very fast overall contraction phase. It is worth noting that the observed MS at each time may differ substantially from the ZAMS mainly for those stars ($M \gtrsim 1.2 M_\odot$) whose core H-burning lifetime is shorter than the age of the typical host galaxy. In this mass range, the MS of a composite stellar population appears as a relatively wide band whose sharp blue edge corresponds to the ZAMS and whose red edge marks the beginning of the rapid redward evolution following exhaustion of H in the core. Hence, the distribution of stars on the MS is determined by the IMF and by the evolution rate along the off-ZAMS tracks.

More massive stars have shorter MS lifetimes and, at fixed Z , leave the MS at higher luminosities. This is used to determine ages of star clusters, and it allows a determination of the range of ages present in a galaxy with little ambiguity (Figure 1). An indication of metallicity can be obtained from the MS itself: for a given He content (see Norris 2004), its color depends quite strongly on metallicity, in such a way that the whole CMD maintains its shape but gets shifted to the red as metallicity increases. In particular, the position on the MS below the oldest turnoff stars depends very little on age, and thus its red and blue edges ideally provide an indication of the maximum and minimum metallicity present in the galaxy. The MS, however, is not totally exempt from the so-called age, metallicity degeneracy,

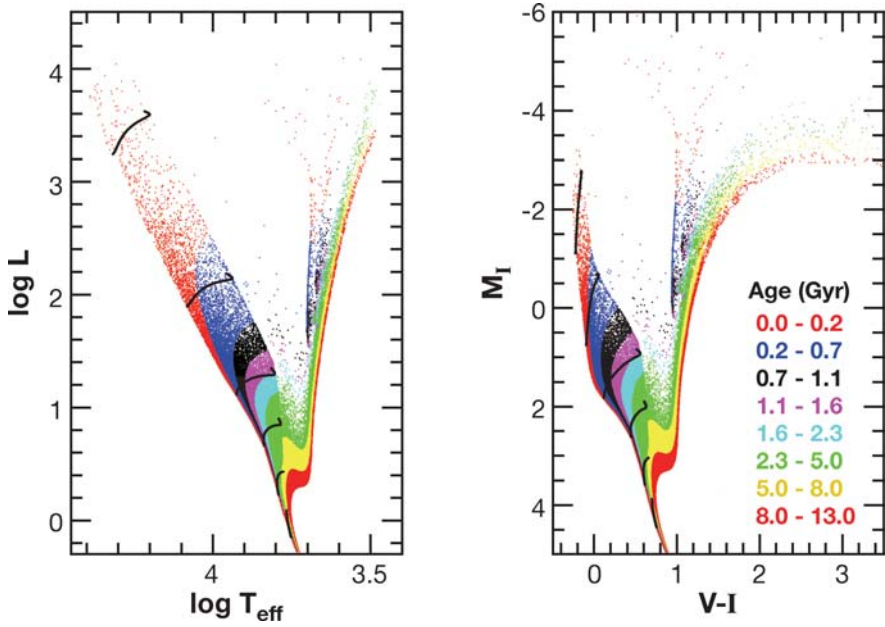


Figure 1 Synthetic color-magnitude diagram (CMD) showing the position of stars in different age intervals in the theoretical (*left*) and the observational (*right*) plane. The Teramo stellar evolution models have been used in the computation. Constant SFR from 13 Gyr ago to the present time, $Z = 0.0198$, IMF slope $\alpha = -2.3$ and no binaries have been assumed. MS stellar evolutionary tracks for stars of masses 7, 3, 1.9, 1.5, 1.2, and 1 M_{\odot} have been superimposed.

which dramatically affects other evolutionary phases. In this case, at fixed age, a more metal-rich population tends to be fainter and redder just as at fixed metallicity an older one would be.

In summary, the information provided by the MS is the following: (a) By comparing the CMD with theoretical isochrones, one can determine the range of ages and metallicities present. (b) To quantitatively determine the SFH, it is necessary to compare the observed density distribution of stars with that predicted by stellar evolution (see Section 4.7). (c) Because, below the oldest MS turnoff, we find unevolved low-mass stars of any age, the corresponding luminosity function (LF) depends only on the mass–luminosity relation (which depends weakly on metallicity and He content) and the IMF. Given an empirical or theoretical determination of the mass–luminosity relation, the IMF can be obtained from the LF.

In this section, we discuss the main uncertainties affecting the position and lifetime of stars on the MS, which are responsible for much of the difference between stellar evolution libraries. These include the treatment of convective core overshooting and diffusion, and the effect of chemical composition (He, α elements, and metallicity).

4.1. Comparison of MS Predictions Among Different Models

4.1.1. THE POSITION OF THE MS STARS ON THE CMD Figure 2 shows a comparison between the Teramo (set with overshooting), Girardi, Geneva, Pisa, Y^2 and Pols isochrones (see Table 1). For this comparison, we have chosen to vary the age of the models represented in order to approximately reproduce the same turnoff and subgiant-branch loci. This provides a direct indication of the difference in the models in terms of age of the population. The metallicity has been fixed at $Z = 0.001$, a typical value for dwarf galaxies. A qualitatively similar behavior has been found both in the theoretical plane and at other metallicities, including $Z = Z_{\odot}$, where, due to the solar calibration, the models belonging to different sets are expected to be more similar.

From the *left panel* of Figure 2, we conclude the following. All models except the Teramo reproduce the same M_V^{TO} with similar ages. Teramo's models require significantly larger ages, 0.8 and 3 Gyr, respectively, to reproduce the ~ 0.5 and ~ 2 Gyr turnoffs of the other sets. The discrepancy disappears both for older (~ 14 Gyr) and younger (~ 0.1 Gyr) ages. Differences in the shape of the turnoff region are only evident for ages ~ 2 Gyr, mainly reflecting different

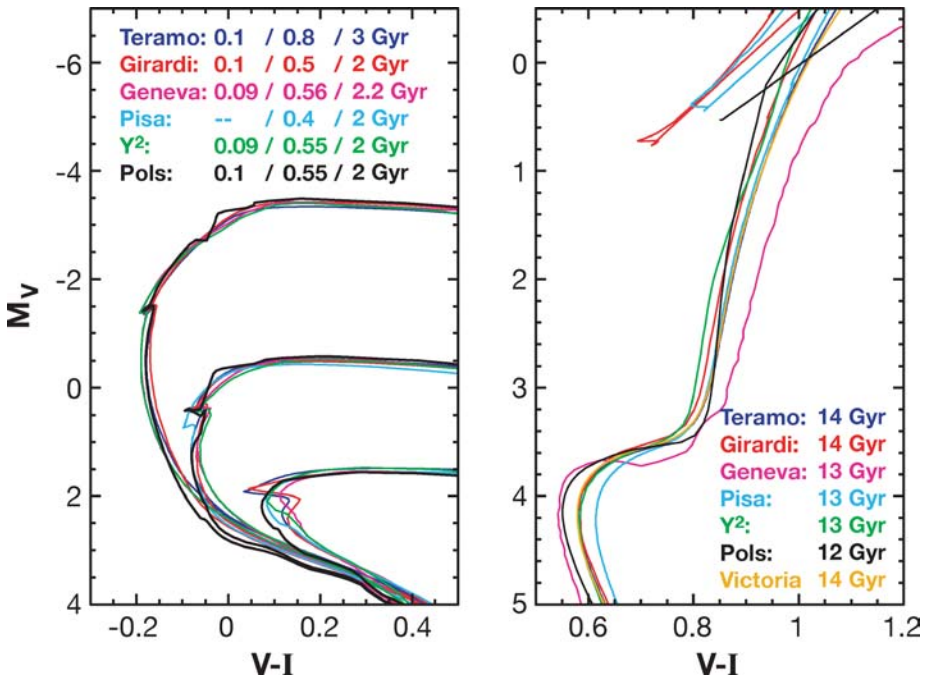


Figure 2 *Left:* Young and intermediate-age isochrones from different libraries. Old models are shown with an expanded scale in the right panel. See text for details.

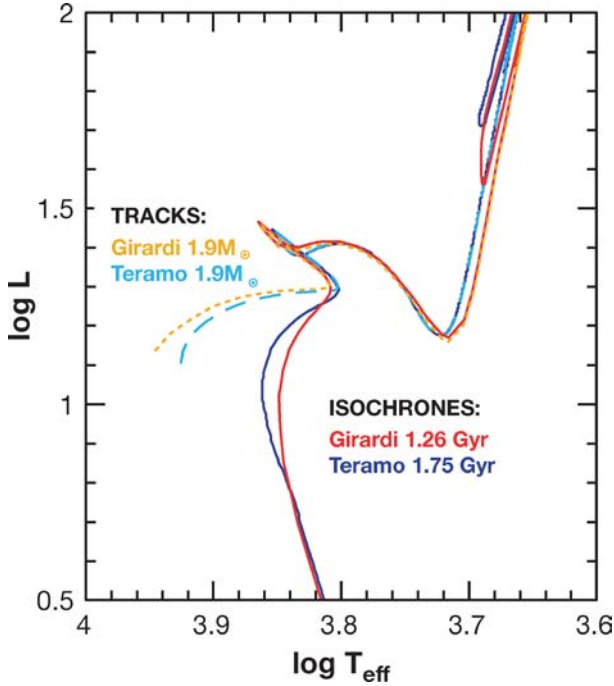


Figure 3 *Dashed lines:* Tracks of identical mass from the Teramo and Girardi libraries. *Solid lines:* Isochrones of ages corresponding to the lifetimes of each track at the point of core H exhaustion. Note that in spite of different ages, the isochrone shapes are very similar.

prescriptions adopted to decrease the extent of overshooting with decreasing mass in this mass range (Section 4.2). For the old populations (*right panel*), predicted ages are within ± 1 Gyr of each other. The Pisa and Y^2 models are the only ones to include diffusion, and both are among those requiring an isochrone 1 Gyr younger than most others, as expected.

The intermediate-age discrepancy between the Teramo and other models deserves a closer examination. In Figure 3, two tracks of identical mass from the Teramo and Girardi libraries are represented. They occupy very similar loci in the CMD, implying a very similar mass–luminosity relation (see Section 4.1.2). However, their turnoff ages are quite different (1.75 and 1.26 Gyr respectively). In other words, the two libraries would assign very similar masses but different ages to a given MS star. Pietrinferni et al. (2004) investigated the possible origin of this discrepancy and concluded that only a fraction of it is related to differences in the overshooting treatment. The rest has to be ascribed to the input physics (see also Supplemental Figure 1; follow the Supplemental Material link from the Annual Reviews home page at <http://www.annualreviews.org/>).

4.1.2. THE STAR COUNTS ON THE MAIN SEQUENCE Let us consider a single-age, single-metallicity stellar population observed at the moment in which all its stars are on the ZAMS. For a given chemical composition, the LF of such a system would depend only on the IMF and the ZAMS mass–luminosity relation. In practice, the restriction of a single age can be relaxed, provided that the mass of the stars is low enough so that evolution off the ZAMS is negligible. This allows us to retrieve the IMF of a stellar system from the LF below the oldest MS turnoff, under the assumption of a particular mass–luminosity relation. The latter can be determined empirically (e.g., Henry & McCarthy 1993, Delfosse et al. 2000, Malkov 2003) or from stellar evolution models, in which case it would depend on their input physics.

Above the oldest MS turnoff of a composite stellar population, the distribution of stars on the MS for a given SFH depends also on their lifetimes during the MS evolution. For example, the evolutionary rate of an intermediate-mass star is slower near the ZAMS, and therefore, in a system that has experienced a constant SFR, the density of stars there is larger. In addition, different stellar evolution libraries may predict, for the same SFH, a different density of stars at each luminosity. This will certainly be the case for the Teramo and Girardi libraries. To take the example on Figure 3, the Teramo models will predict, for the same SFH, a larger density of stars along the $1.9 M_{\odot}$ track than the Girardi models, because their evolutionary rate is slower (a $1.9 M_{\odot}$ star takes 1.75 Gyr to exhaust the hydrogen in its core, compared to 1.25 Gyr in the Girardi model). In contrast, the LF of the unevolved MS reflects changes of the slope of the IMF and the mass–luminosity relation. For a realistic power-law IMF (e.g., Kroupa 2001), the MS LF shows a change of slope at $M_V \sim 2$ (the exact value depends on Z), uniquely determined by the inflection in the mass–luminosity relation that is in turn introduced by the bolometric corrections. The theoretical mass–luminosity relation from the two model libraries with the largest differences, i.e., the Girardi and Teramo models, agree well, being always within $< 20\%$ of each other (see also Supplementary Figure 2; follow the Supplemental Material link from the Annual Reviews home page at <http://www.annualreviews.org/>).

4.2. The Effect of Core Convective Overshoot

In stars of $M \lesssim 1 M_{\odot}$ (the exact value depends on Z), core H burning occurs in radiative conditions, whereas more massive stars develop a convective core. The formal boundary of the convective core in canonical stellar evolution models is set by the Schwarzschild criterion, where the acceleration of the convective cells vanishes. It seems, however, sensible that the actual size of the core is somewhat larger and that it extends up to where the velocity of the convective cells is zero. The length of this further extension (overshoot) remains conjectural and is parameterized in different ways, usually after calibration with observations. However, this tuning of overshooting erases differences in the core size due to other factors, e.g., (a) the input physics used to calculate the radiative and adiabatic temperature

gradients defining the size of the convective region, and (b) the increase of the core size as a consequence of rotationally induced mixing.

The extension of the region affected by the extra mixing is usually defined in terms of a parameter, λ_{OV} , which gives the length, expressed as a fraction of the local pressure scale height, H_p , traveled by the convective cells outside the formal convective boundary. The net effect of the inclusion of overshooting is an increase of the core mass. Models calculated by taking into account convective core overshoot reach higher luminosities (see Supplementary Figure 3; follow the Supplemental Material link from the Annual Reviews home page at <http://www.annualreviews.org/>) and live longer on the MS than classical models. The core He-burning lifetime, however, is modestly decreased. Therefore, interpreting a given set of observations using models calculated with convective core overshoot would result in older ages than those derived with canonical models. Pietrinferni et al. (2004, their figure 1) show that the turnoff morphology of populations a few Gyr old depends not only on the amount of overshooting assumed but also on the prescription adopted to decrease the extent of overshooting with decreasing mass, which varies between libraries (see also Supplementary Figure 4; follow the Supplemental Material link from the Annual Reviews home page at <http://www.annualreviews.org/>).

4.2.1. OBSERVATIONAL EVIDENCE OF CONVECTIVE CORE OVERSHOOT It might be argued that the presence of some overshooting is expected by definition, but the problem is *how much*. The precise quantity of overshooting is, however, strongly dependent on the model, because the nominal size of the core (with $\lambda_{OV} = 0$) depends on the other input physics. Hence, in general, the amount of overshoot needed for one set of models to match the observations may not be valid for another set.

Most empirical tests of the existence of core convective overshoot have relied on observations of Galactic open clusters. In general, they have reached the conclusion that a certain amount of overshooting is required to reproduce the CMDs for metallicities close to solar. The reader is referred to Maeder & Meynet (1989) and Stothers (1991) for early references and a critical discussion of the observable features sensitive to overshooting (see also Chiosi, Bertelli & Bressan 1992; Rosvick & VandenBerg 1998; Woo & Demarque 2001). The Magellanic Clouds offer the opportunity to test whether there is a dependence of overshooting with metallicity. A number of *young* Magellanic Clouds clusters have been used to constrain evolutionary models of young stars, often with contradictory results. In particular, there is a long-lasting debate about NGC 1866 (see Brocato et al. 2003 for a summary). As for intermediate-age LMC clusters, Gallart et al. (2003), Woo et al. (2003) and Bertelli et al. (2003) studied a set of LMC clusters in the 1–3 Gyr interval with the Y^2 and Girardi libraries. In the range of masses explored (1.2–2 M_{\odot}), reasonable agreement was found with the current prescriptions of these models. Finally, Cordier et al. (2002) introduced a method to estimate the amount of overshooting using field star data in the LMC and SMC. They found

indications of a possible metallicity dependence (larger overshooting as metallicity decreases).

Studies of detached eclipsing binaries can also constrain λ_{OV} by direct comparison with stellar tracks in the $[\log T_{\text{eff}} - \log g]$ plane (Schroder, Pols & Eggleton 1997; Ribas, Jordi & Giménez 2000), and the results generally agree with those from cluster observations. They also provide some evidence that λ_{OV} increases with stellar mass from 0.1 for $M \simeq 1.3 M_{\odot}$ up to very large values $\simeq 0.6$ for $M \simeq 10 M_{\odot}$. Ribas, Jordi & Giménez (2000) also found indications for some variation of λ_{OV} with metallicity, such that lower values are inferred for sub-solar metallicities. Studies of the masses and luminosities of bump Cepheids (Bono, Castellani & Marconi 2002; Keller & Wood 2002) also found support for $\lambda_{OV} > 0$. Finally, astroseismology has provided support for the inclusion of overshooting in models of massive stars (Aerts et al. 2003, Dupret et al. 2004), even though the amount estimated by these authors for a star of $\simeq 10 M_{\odot}$ is lower than that estimated for eclipsing binaries of similar masses.

4.3. Helium and Heavy Element Diffusion

The term microscopic diffusion is used to refer to the process of element settling and consequent chemical stratification. Radiative levitation, which acts in the opposite direction (radiation pushing toward the surface ions with large cross-sections), can also contribute to this process. Both microscopic diffusion and radiative levitation are slowed down by collisions between particles and by convection. Diffusion is efficient only for stars with lifetimes long enough to allow gravity to produce element sedimentation, i.e., low-mass stars during H burning and hot HB stars (Behr et al. 1999). Low-metallicity stars have smaller convective envelopes, and thus the effect of diffusion is expected to be larger. However, it is known from helioseismological constraints that microscopic diffusion is at work in the Sun (Christensen-Dalsgaard, Proffitt & Thompson 1993; Basu, Pinsonneault & Bahcall 2000).

The efficiency of atomic diffusion in low-mass, metal-poor stars is under debate due to the evidence that theoretical predictions cannot successfully reproduce spectroscopic measurements for turnoff stars in galactic GCs (Gratton et al. 2001). Chaboyer et al. (2001) and Richard et al. (2002) have proposed two alternative reconciling scenarios. The first invokes rotationally induced mixing in the surface layers, which would suppress diffusion in them. The second uses sophisticated modeling to include self-consistently the effects of the diffusion of metals with their radiative accelerations.

Although the efficiency of diffusion is still debated, its impact on the interpretation of the CMDs of galaxies is not dramatic. The inclusion of diffusion in stellar evolution models reduces the MS lifetimes and the effective temperatures of the stars. This produces a shift of the MS turnoff toward fainter magnitudes, by 0.05–0.2 mag, depending on the assumed efficiency. Such a difference produces an appreciable difference in age only for old populations, where it can reach a maximum of ~ 1 Gyr at ~ 15 Gyr (Castellani & Degl’Innocenti 1999).

4.4. α -Element Enhancement

The α elements (O, Mg, Si, S, Ca, Ti) are often more abundant, with respect to Fe, than in our Sun. In almost all components of the Milky Way, metal-poor stars have $[\alpha/\text{Fe}] \sim 0.3$ reaching as high as $[\alpha/\text{Fe}] \sim 0.5$ in the most metal-poor tail ($[\text{Fe}/\text{H}] \sim -2.0$; Lee & Carney 2002). The Galactic disk shows a decline of $[\alpha/\text{Fe}]$ starting at $[\text{Fe}/\text{H}] \sim -1$ and reaching the solar value at $Z = Z_{\odot}$. However, though GC stars are α enhanced at all metallicities, dSphs seem to have low $[\alpha/\text{Fe}]$ over their whole metallicity range. The reader is referred to McWilliam (1997) and to Bensby, Feltzing & Lundström (2004) for the Galactic thick and thin disk, McWilliam & Rich (2004) for the Galactic Bulge, Lee & Carney (2002) for the GCs, and Venn et al. (2004) for dSphs. In the interpretation of the CMDs of external galaxies, the fact that the chemical patterns, due to their dependence on the SFH, may be unknown or different from those found in the Milky Way, is an additional difficulty.

The location of the MS and the shape of the isochrones is affected by the relative abundance of heavy elements and, in particular, of the α elements. A change in their abundance with respect to Fe affects the stellar luminosities and temperatures, because it changes the radiative opacity and, in the case of O, the efficiency of nuclear reactions. Salaris, Chieffi & Straniero (1993) demonstrated that isochrone features depend substantially on the abundances of the nine most abundant elements, and in particular on the ratio of the high (C, N, O, Ne) over the low (Mg, Si, S, Ca, Fe) ionization potential elements. They showed, however, that α -enhanced models are well mimicked by the standard scaled solar ones of the same global metallicity¹ up to $[\text{Fe}/\text{H}] \sim -0.8$. For higher metallicities, α -enhanced models begin to have systematically hotter turnoffs and RGBs compared to the scaled solar ones.

VandenBerg et al. (2000) calculated a set of α -enhanced isochrones (age > 8 Gyr, $-2.3 < [\text{M}/\text{H}] < -0.8$), assuming uniform enhancement for all the α elements and $[\alpha/\text{Fe}] = 0.3, 0.6$. The complementary work of Salasnich et al. (2000) offers an extended grid of models (ages: 0.01–16 Gyr, $-0.4 < [\text{M}/\text{H}] < +0.6$), where α elements have different relative abundances, according to the observations of metal-poor stars by Ryan, Norris & Bessell (1991). Both indicate that, at high metallicities, the differences between α -enhanced and scaled solar isochrones are almost exclusively in color. They are larger at older ages ($\Delta \log T_{\text{eff}} = 0.011$ at 10 Gyr) and decrease to a negligible effect at ~ 0.1 Gyr. The luminosities of MS turnoff, subgiant branch, and of the tip of the RGB are nearly unchanged by varying α enhancement except in the intermediate-age

¹For a Ross & Aller (1976) solar chemical mixture, the relation between the total metallicity and iron abundance is expressed as a function of α enhancement is $[\text{M}/\text{H}] = [\text{Fe}/\text{H}] + \log(0.638 \times 10^{[\alpha/\text{Fe}]} + 0.362)$. Adjustments should be applied (see Yi et al. 2001 for an alternative relation) for more recent, sometimes substantially different (see Asplund, Grevesse & Sauval 2004 and references therein) determinations of the solar metal distribution.

regime, where α -enhanced isochrones are slightly fainter than scaled solar ones.

4.5. Effect of Metallicity on ZAMS Colors

The color width of the low MS of a population is potentially a robust indication of its spread in metallicity. This is a consequence of the solid prediction that, as the metallicity increases, the opacity is larger and therefore the stars occupy fainter and redder loci. However, in the few years after the release of the *HIPPARCOS* catalog, there has been much discussion about how solid this prediction is. Three almost simultaneous papers made contradictory claims. Reid (1999) constructed the CMD of two samples of disk and halo dwarfs; the disk dwarfs were found to be in good agreement with the Bertelli et al. (1994) and the halo dwarfs were in good agreement with D'Antona, Caloi & Mazzitelli (1997) isochrones. However, Lebreton (2000) concluded instead that though metal-rich subdwarfs were very well reproduced by current stellar models (Victoria), the metal-poor sample was definitely too red, pointing toward a worrying independence of the ZAMS color on metallicity. But then Kotoneva, Flynn & Jimenez (2002) claimed that most isochrones reproduced reasonably well the CMD distribution of metal-poor subdwarfs, whereas the metal-rich end was not well matched. Other studies confirmed the agreement found by Reid (1999), however they analyzed only a limited metallicity range (e.g., VandenBerg et al. 2000, Pietrinferni et al. 2004; in the metal-poor and metal-rich regime, respectively).

Several new measurements of the metallicity and colors of a large fraction of the *HIPPARCOS* subdwarfs have recently been made available (Gratton et al. 2003; Percival et al. 2002). Using these, we have constructed the CMD in Figure 4. The sample comes from Gratton et al. (2003) for the metal-poor stars, and from Percival et al. (2002) for the metal-rich ones. Gratton et al. (2003) obtained spectroscopic abundances, including α enhancement, whereas Percival et al. (2002) derived $[\text{Fe}/\text{H}]$ from Strömgren photometry and subsequently converted these photometric metallicities to the Carretta & Gratton (1997) scale using the transformations by Clementini et al. (1999). For each star in the Gratton sample, we calculated the total metallicity, $[\text{M}/\text{H}]$, from $[\text{Fe}/\text{H}]$ and $[\alpha/\text{Fe}]$. For the Percival sample, we assumed zero α enhancement, given that the Gratton et al. measurements indicated that the $[\alpha/\text{Fe}] \simeq 0$ at $[\text{Fe}/\text{H}] \sim -0.1$. The stars were divided into bins of global metallicity and compared to the relevant isochrones from the Teramo set. The agreement was very good at all metallicities. A very similar result would be obtained with the Girardi models.

We believe that the origin of the controversy was a combination of poorly measured abundances and (possibly) inconsistent treatment of the α enhancement. Indeed, the latter has the effect of changing the metallicity trend in the sense that a star with $[\text{Fe}/\text{H}] = -0.8$ and $[\alpha/\text{Fe}] = +0.3$ has the same global metallicity (hence *roughly* the same position in the CMD) as one of $[\text{Fe}/\text{H}] = -0.6$ and $[\alpha/\text{Fe}] = 0$. This effect, if not properly taken into account, may have led to the conclusion that

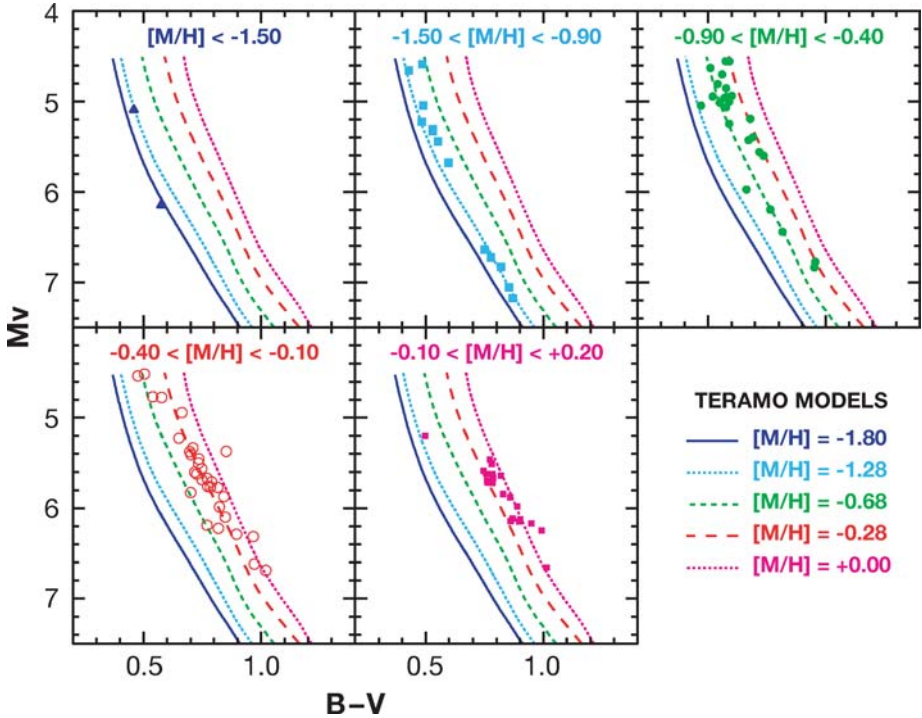


Figure 4 Comparison between the observed CMD locations of *HIPPARCOS* subdwarfs and theoretical isochrones of the Teramo set at different metallicities. See text for details.

there was little change in the subdwarf ZAMS color with increasing metallicity for $[\text{Fe}/\text{H}] > -1$.

4.6. Uncertainties in the He Enrichment Law

The initial He abundance, Y , adopted in a stellar evolution model substantially affects the luminosity and therefore the lifetime of MS stars. The effect of changing the He abundance in stellar evolution models is relatively well known. Everything else being constant, an increase in the He content increases the effective temperature and luminosity, and decreases the MS width (Claret 1995) (see also Supplemental Figure 5; follow the Supplemental Material link from the Annual Reviews home page at <http://www.annualreviews.org/>). However, most grids of stellar evolution models are calculated for a broad range of metallicities, but each one assumes a particular $\Delta Y/\Delta Z$ (see Table 1), with only one value of He assumed for each Z (see Claret & Giménez 1998 and companion papers for models at constant Z and varying Y).

The uncertainties are related to the fact that the Y -to- Z enrichment ratio ($\Delta Y/\Delta Z$) is not well known and probably not unique (e.g., Norris 2004). In spite of this, Y is generally assumed to vary with Z as $Y = Y_p + (\Delta Y/\Delta Z)Z$, where Y_p is the

primordial He. (Y_{\odot} , Z_{\odot}) is assumed as a second fixed point. Current empirical estimates of Y_p based on measurements in low-metallicity extragalactic HII regions agree within $\simeq 5\%$ with Y_p in the range of 0.230–0.242 (see Olive, Steigman & Skillman 1997; Luridiana et al. 2003; Izotov & Thuan 2004). Cassisi, Salaris & Irwin (2003) obtain $Y_p = 0.243 \pm 0.006$ using the R parameter² on GCs, and models with improved $^{12}\text{C}(\alpha, \gamma)^{16}\text{O}$ reaction rate (Kunz et al. 2002) and equation of state (Irwin 2005). Both are consistent with values of Y_p derived from detailed big bang nucleosynthesis calculations using current cosmic microwave background results: $Y_p = 0.2479 \pm 0.0004$ (Coc et al. 2004). Paradoxically, the values (Y_{\odot} , Z_{\odot}) are quite uncertain if one considers the new measurements of the oxygen abundance (lower by a factor of $\simeq 1.5$ than classically assumed values) obtained by Asplund et al. (2004) and Meléndez (2004). Assuming these, Basu & Antia (2004) derive $Y_{\odot} \simeq 0.2486$. We then have (Y_{\odot} , Z_{\odot}) = (0.2486, 0.0122). These are substantially different from currently accepted values (Y_{\odot} , Z_{\odot}) \simeq (0.28, 0.018); see Table 1. Note that the new values for the Sun would imply a very small He enrichment over almost 10 Gyr of Galactic chemical evolution. Salaris et al. (2004) may have noted a related effect, an independence of the He content on metallicity in GCs in a wide range of metallicities. In view of this complicated situation, it would be highly desirable that stellar evolution libraries provide different values of Y for each Z , thus giving users the possibility of evaluating the impact of different He enrichment laws in the study not only of galaxies but also of star clusters, where there seems to be evidences of self-enrichment in at least some cases (D’Antona & Caloi 2004).

4.7. A Closer Look to the Derivation of the SFH from the Main Sequence

Here we critically assess the power and limitations of MS luminosity and color functions to retrieve the SFH of a galaxy. The combination of both may be preferred (e.g., Gallart et al. 1999a, Brown et al. 2003).

A number of analyses based on the MS LF exist, especially for the LMC (Holtzman et al. 1997, Smecker-Hane et al. 2002; see also Mighell & Butcher 1992). The slope of the LF and the number of stars in different magnitude bins, compared with the same information obtained from synthetic CMDs, are the two diagnostics typically used. Slope variations in the LF are sometimes interpreted as an indication of periods of enhanced star formation. However, they also occur in smoothly varying SFHs (e.g., Figure 5a) and the effects of small number statistics can be dramatic in simulating them.

Figure 5 shows the effects on the MS LF of exponentially varying $\text{SFR}(t)$. Note that large changes in the SFR exponential scale are only reflected as slight LF slope changes (the LF slope in the magnitude range $M_I = 0-2.8$ varies only from 0.60 to 0.77 for the extreme cases $\tau = -5$ to $\tau = 5$, respectively, being 0.65

²The R parameter is defined as the number ratio of HB to RGB stars brighter than the HB (Iben 1968).

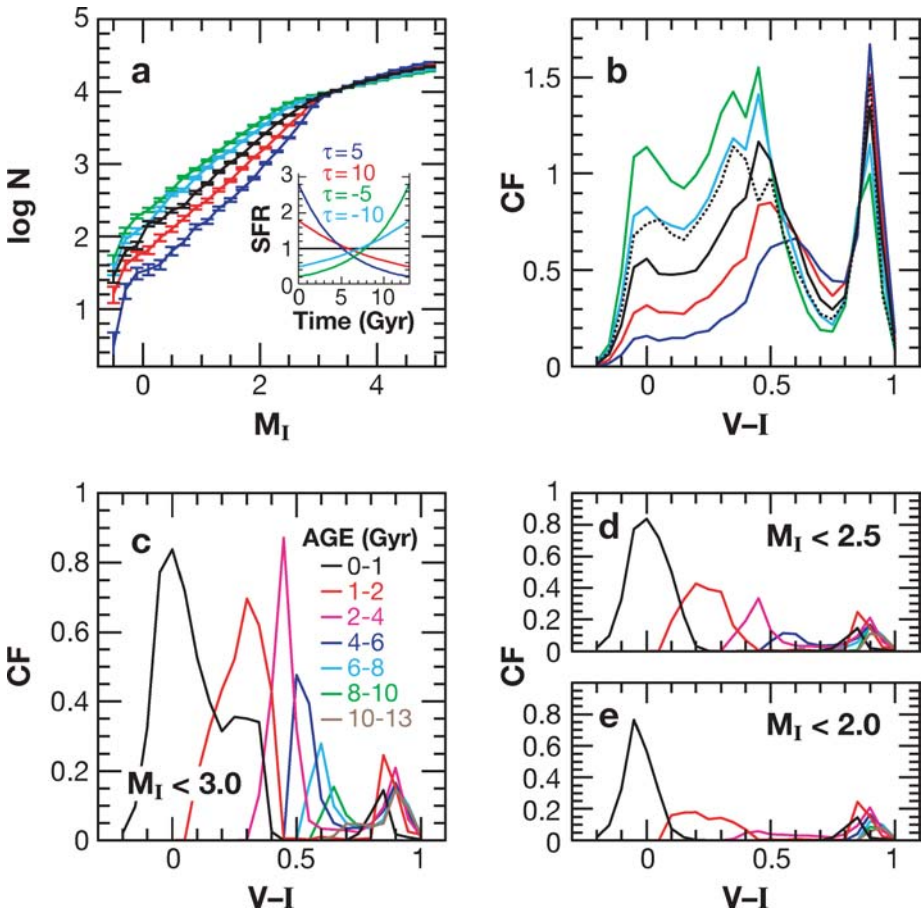


Figure 5 Effects of $SFR(t)$ changes on (a) the MS LF and on (b) the MS color function (CF, integrated in the range $-2 \leq M_I \leq 3.5$) as computed using the Girardi library and assuming constant $Z = 0.004$ and Kroupa (2001) IMF. Constant and exponential $SFR(t)$ ($\propto e^{-(t/\tau)}$, with $\tau = 10, 5, -5, -10$) have been assumed, as shown in the inset, where t is the age of the stellar system. In (b), a constant $SFR(t)$ population computed using the Teramo models (black dotted line) is plotted for comparison. (c) MS CF of stellar populations with limited age range, as described in the labels. (d, e) Effect of the CMD limiting magnitude (labeled) on the possibility of retrieving information on populations of different ages. The Girardi library with constant $SFR(t)$ and the above population parameters have been used in (c), (d), and (e). Synthetic CMDs with 2×10^5 stars have been used in all cases, and arbitrary normalizations applied. [*]

Annu. Rev. Astro. Astrophys. 2005.43:387-434. Downloaded from www.annualreviews.org by University of Maryland - College Park on 07/15/12. For personal use only.

for a constant SFR). This is unlikely to be detected in real CMDs. Small changes in the metallicity law have a negligible effect on the LF slope. In the case of a bursting SFR(t), slope changes may be more noticeable if a significant increase in the SFR(t) occurred in the last half of the lifetime of the galaxy.

The pattern followed by the distribution of stars of different ages on the MS (see Figure 1) suggests that the MS color function could be a better tracer of the SFH. The fact that the turnoffs of younger stellar populations are hotter, and therefore bluer, than those of older populations (see Figure 1), implies a general dependency on age of the color function of the MS and subgiant-branch stars brighter than the oldest MS turnoff. In addition, as discussed in the introduction of Section 4, stars with $M \gtrsim 1.2 M_{\odot}$ evolve at almost constant luminosity and decreasing temperature while on the MS. Therefore, stars located along lines of constant luminosity have very similar masses but a range of ages. This property has been used to obtain information on the SFH for a limited age range, in a way which is almost independent of variations of the IMF (Gallagher et al. 1996; Elson, Gilmore & Santiago 1997).

Figure 5*b* shows the MS color function of populations with the same varying SFR(t) as Figure 5*a*. Note that the differences among the SFRs are obvious with this representation (see also Supplemental Figure 6; follow the Supplemental Material link from the Annual Reviews home page at <http://www.annualreviews.org/>). Figure 5*c* shows which populations contribute to each feature in the color function, and how information on older populations disappears from shallower CMDs (Figure 5*d,e*). Whereas populations as old as 10 Gyr contribute to the color function in a CMD reaching the oldest MS turnoffs, at $M_I \simeq +3$, only populations up to 6 and 2 Gyr are relevant in a CMD 0.5 and 1 mag shallower. This demonstrates the importance of obtaining CMDs reaching the magnitude of the oldest MS turnoffs, to allow information on the whole SFH of the galaxy to be obtained.

5. THE RED GIANT BRANCH

During the RGB phase, low-mass stars ($M < M_{\text{HeF}}$) burn H in a shell, building an electron-degenerate He core while climbing the RGB close to the Hayashi line. For them, the RGB lifetime and magnitude extent on the CMD is much larger than for intermediate-mass stars. For this reason, the M_{HeF} limit marks the so-called “RGB phase transition” (Sweigart, Greggio & Renzini 1990). Because of its luminosity, the RGB is the only window into the study of the old and intermediate-age population in distant galaxies.

The position of the RGB on the CMD depends mainly on metallicity, such that more metal-rich stars are redder, and less strongly on age, such that older stars are also redder. Because chemical evolution is such that, in general, younger stars have higher metallicity than older ones, age may partly counteract the effect of metallicity on the RGB color. This double dependence on metallicity and age is the origin of RGB age–metallicity degeneracy, which is partially responsible for

the limited amount of information that can be retrieved from the RGB. Finally, though age shifts the RGB without heavily altering its shape, metallicity has a stronger effect on the RGB shape and/or slope (see also Supplementary Figure 7; follow the Supplemental Material link from the Annual Reviews home page at <http://www.annualreviews.org/>).

The strong dependence of the RGB color on metallicity is the reason for one of the most widespread practices for retrieving the stellar metallicity distribution of a nearby galaxy, which uses the distribution of stars on the RGB. The change in the shape of the RGB with metallicity has also been proposed as a metallicity indicator for single-age populations. Both techniques are discussed in Section 5.3. In addition, the RGB contains stars formed over most of a galaxy's history. The number of stars populating this phase is, therefore, a potentially accurate indicator of the mean SFR of a galaxy at intermediate and old ages. The detailed distribution of stars along the RGB has also been used in global fits of the CMD, to retrieve SFHs through the comparison with synthetic CMDs. A particular feature on the RGB LF, the RGB-bump, has been used as a metallicity indicator in galaxies with a predominately old stellar population (Majewski et al. 1999, Monaco et al. 2002). Finally, the luminosity at the brightest point (tip) of the RGB is remarkably constant for ages older than a few Gyr and thus is used as a standard candle (Section 5.4).

In this section, we discuss some important ingredients affecting the RGB position on the CMD and its use as a metallicity or SFR indicator. We refer the reader to Salaris et al. (2002) for a recent review on the current status of RGB modeling.

5.1. The RGB Position in the CMD

5.1.1. COMPARISON AMONG DIFFERENT MODELS Figure 6 shows a comparison of the RGB loci predicted by different models. The figure inset allows a more quantitative comparison of the variation of the RGB color at $M_I = 1.5$ as a function of metallicity for a larger number of models. We compare the RGB color at a level where the bolometric corrections are relatively robust (see Section 5.1.3), and most of the differences are due to the adopted mixing length or, in general, to the model input physics. The largest differences occur at $Z = Z_\odot$, although it is precisely at this metallicity that the mixing length is calibrated (see Section 5.1.2). This shows that although at $Z = Z_\odot$ all the models coincide on the MS (a consequence of the solar calibration), this is not necessarily true for the RGBs. At $M_I = 1.5$, differences are as large as $\Delta(V - I) = 0.13$, and they are larger at brighter magnitudes, where the RGB is usually used to measure metallicities. The dispersion of model predictions can be taken as a lower limit on the "intrinsic error" of the absolute RGB color. The total spread in color for the whole metallicity range is also model dependent. In particular, the Girardi models predict $\Delta(V - I) = 0.4$ going from $[M/H] = -2.5$ to $[M/H] = +0.2$, whereas the Pols models predict $\Delta(V - I) = 0.23$ for the same metallicity range. This shows that RGB color predictions should be taken with care.

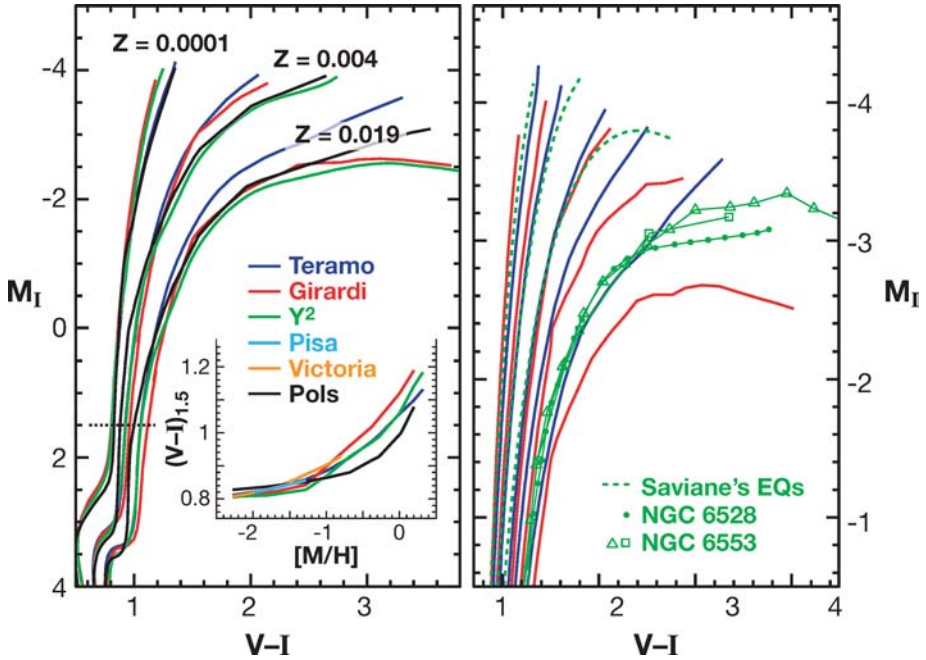


Figure 6 (Left) RGB isochrones at 14 Gyr from different libraries. The *inset* shows the run of the RGB color (at $M_I = 1.5$, *dotted line*) as a function of metallicity. The Pisa models are not clearly visible because they fall on top of the Teramo ones. (Right) Theoretical RGBs by Teramo and Girardi (for $Z = 0.0001, 0.001, 0.004, 0.008, 0.019$) compared with empirical data. *Green dashed lines* represent Saviane et al. (2000) hyperbolas, and *symbols* represent fiducial lines for NGC 6528 (Feltzing & Johnson 2002, *filled circles*) and NGC 6553 (Ortolani et al. 1995, *squares*; Sagar et al. 1999, *triangles*).

5.1.2. THE MIXING LENGTH One of the largest uncertainties in stellar evolution models comes from the treatment of convective fluxes. The most common way to model convection is through the mixing length theory (Bohm-Vitense 1958). It relies on a single free parameter, α_{MLT} , defined as the ratio of the mixing length to the pressure scale height. The value of α_{MLT} determines the efficiency of convection, and it has to be calibrated empirically. A change in the mixing-length parameter affects those regions of the CMD where stars have a convective envelope, namely the MS of low-mass stars and the RGB. Specifically, a change of 30% in the adopted value for α_{MLT} changes the color of the MS by $\Delta(B - V) \approx 0.017$ and of the RGB by $\Delta(B - V) \approx 0.045$ (Cariulo et al. 2004).

One robust calibration point for the mixing length is our Sun: the value of α_{MLT} has to be such that a star with $M = 1 M_{\odot}$ and $L = 1 L_{\odot}$, and current (i.e., at age 4.5 Gyr) $Z = Z_{\odot}$ and $Y = Y_{\odot}$, has $R = R_{\odot}$. Note that, due to slightly different implementations of the theory and different input physics, the

precise value of α_{MLT} varies from model to model (see Table 1). Though the Sun is a very reliable calibrator, there are no *a priori* reasons to believe that the same mixing length parameter should be valid also for giant stars (Robinson et al. 2004) or for metallicities other than solar. In the past, the value of α_{MLT} suitable for the Sun did not provide a good fit to metal-poor stars (e.g., Vandenberg 1992). This was an argument for calibrating the mixing length with Groombridge 1830, a Population II subdwarf of known radius (Vandenberg 1992), or with some GC RGBs, allowing for the adjustment of α_{MLT} with metallicity (e.g., Chieffi, Straniero & Salaris 1995). In their comparison of observed and theoretical RGB colors as a function of metallicity, Palmieri et al. (2002) concluded that the observed trend of RGB colors is consistent with models adopting a single, metallicity-independent α_{MLT} . A similar conclusion was obtained by Freytag & Salaris (1999) by means of detailed hydrodynamical simulations.

An alternative treatment of convection is the so-called full spectrum of turbulence (Canuto & Mazzitelli 1991). Its main advantages are that a full spectrum of convective cells is considered (as opposed to the unique “typical” size of the mixing length theory) and that the mixing-length scale is no longer a free parameter. The size of the convective regions is anyway subject to a free parameter, namely the overshooting length, but this affects only the boundary of the convective zone, and its value is not completely arbitrary (Ventura et al. 1998, and references therein). Though the treatment of convection in the framework of the full spectrum of turbulence is substantially more elaborate and potentially more realistic, the predicting power of the resulting models is comparable to the standard ones (see Stothers & Chin 1995 for a comparison of the mixing-length theory and the full spectrum of turbulence in the context of modeling of red giant stars and red supergiants.)

5.1.3. THE BOLOMETRIC CORRECTIONS Bolometric corrections (BCs) are necessary to transform theoretical models to the observational plane or to derive physical parameters (T_{eff} , $\log g$) from observed stellar magnitudes and colors. Though BCs are used over the whole temperature range, the problem of their reliability is of special relevance for RGB and AGB stars, because of our current poor ability to model the spectra of cool giants.

The standard way to obtain theoretical BCs is the following. Model atmospheres provide synthetic spectra for a grid of T_{eff} , $\log g$, and Z . The spectra are convolved with a filter response curve to determine what fraction of the bolometric flux is received through the corresponding photometric band. The zero point of this “relative BC” in the V band is obtained by imposing $BC_V^{\odot} = -0.07$ (Cram 1999), whereas all the other bands are calibrated by requiring the colors of Vega to be zero. The accuracy of this procedure is uniquely determined by the accuracy of the model atmospheres for the stars under analysis. Between 4500 K and 50,000 K, where only atomic lines are present in the spectra, current model atmospheres do a good job. In this range, most of the stellar models are transformed through the ATLAS9 library (Kurucz 1992 and subsequent updates; e.g., Castelli et al. 1997, Castelli & Cacciari 2001). Spectra of stars hotter than 50,000 K are well approximated by

black bodies. Below 4500 K, i.e., $(V - I)_0 \sim 1.2$, the spectra are strongly affected by molecular bands, and this significantly alters the amount of flux transmitted through a filter bandpass. The treatment of molecules in model atmospheres is an extremely complex issue, and at the moment there are no theoretical models able to reproduce the observed spectrum of M giant stars. Hence, to deal with M-giants one can either use empirical BCs or make corrections on the theoretical BCs according to observations.

Empirical BCs for near-infrared bands have been determined by Frogel, Persson & Cohen (1983). Nowadays, the two most used empirical color- T_{eff} calibrations are the ones by Montegriffo et al. (1998) and Alonso, Arribas & Martínez-Roger (1999). Both rely on bolometric flux determinations via integration of multi-band observations, and T_{eff} determinations via the Infrared Flux Method (Blackwell et al. 1990). A third empirical spectral library, specific for M-giants, is the one by Fluks et al. (1994), which includes however only solar metallicity stars. The alternative way to obtain BCs for $T_{\text{eff}} < 4500$ K is to apply a correction to theoretical BCs to satisfy observational constraints. Example of such transformations are given in Lejeune, Cuisinier & Buser (1998) and VandenBerg & Clem (2003). The last was subsequently confirmed by fully empirical color- T_{eff} relations (Clem et al. 2004).

The *right panel* of Figure 6 compares the RGBs from Teramo and Girardi with the hyperbolas proposed by Saviane et al. (2000) as an analytic representation of the observed RGB (see Section 5.3). Because the hyperbolas in $(V - I)$ extended only up to the metallicity of 47 Tuc, we also plot for comparison the fiducial sequences for the (\sim solar metallicity) GCs NGC 6528 and NGC 6553. They should overplot the most metal-rich isochrone of each set. In the metal-poor regime, the models do a good job up to the RGB tip. However, larger differences are present between the two model sets and between each of them and the data for $Z \gtrsim 0.0004$. Note, however, that Galactic metal-rich GCs are all seen projected toward the Bulge, where differential reddening and foreground contamination are quite severe. Hence, only a few of the CMDs available in the literature have an upper RGB sufficiently populated and defined to put reliable constraints on the models.

5.2. The RGB Luminosity Function

Stars along the RGB evolve relatively quickly. As a consequence, the RGB of a simple stellar population consists of stars of very similar masses at different evolutionary stages. The number of stars along the RGB is proportional to the evolutionary rate along that stage; hence the RGB LF is a measure of the rate at which the H-burning shell proceeds toward the exterior of the star and the He-core mass increases. This is directly connected both with the details of the envelope stratification and with the nuclear rates. Because RGB stars are among the brightest of a galaxy, their number has a strong influence on the luminosity-integrated properties of the population.

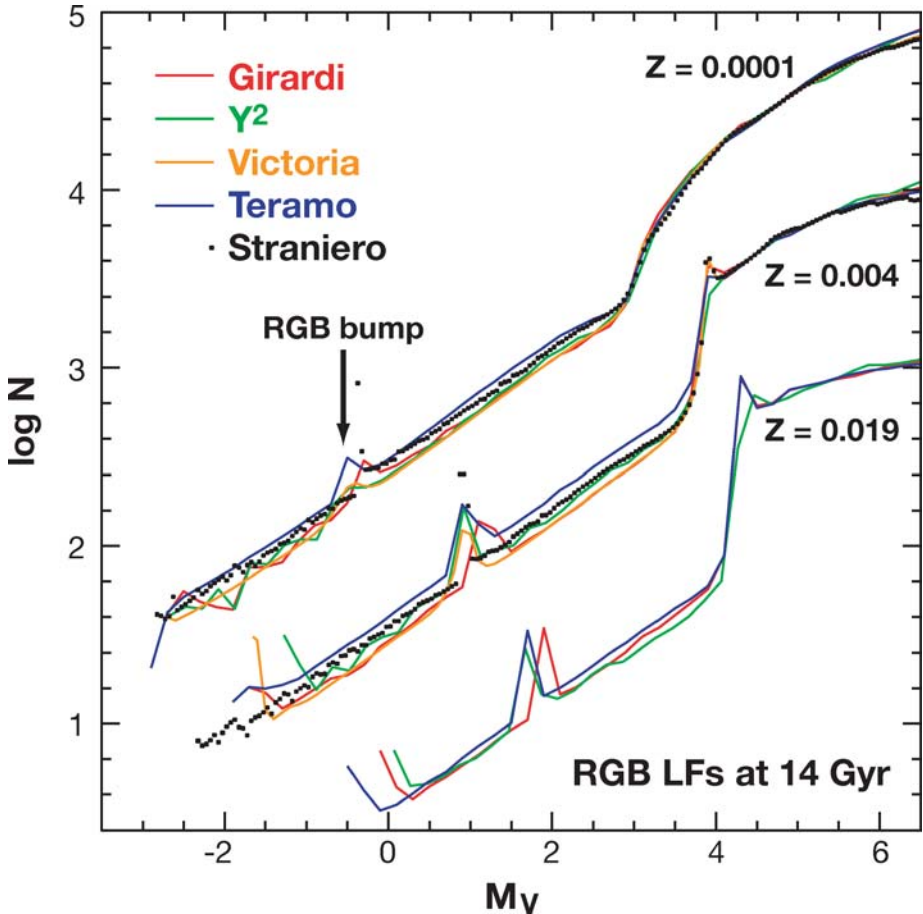


Figure 7 Comparison between theoretical RGB LFs predicted by different models at 14 Gyr and for the three metallicities listed. The RGB LFs were normalized to the total number of MS stars. Small black dots are the Straniero, Chieffi & Limongi (1997) models.

5.2.1. COMPARISON BETWEEN DIFFERENT MODELS In Figure 7, we compare the RGB LF as predicted by different models at fixed old age. The main features visible in the LFs are (a) the steep increase in the number counts around $M_V \sim 4$ coinciding with the horizontal part of the subgiant branch just above the MS turnoff, and (b) the peak in the middle of the RGB: the RGB-bump (Thomas 1967, Iben 1968; c.f., Section 5.2.2). All the LFs were constructed assuming a Salpeter IMF and were normalized to the total number of stars in the two magnitudes below the MS turnoff. *Small black dots* on Figure 7 are the Straniero, Chieffi & Limongi (1997) models. They are shown as a reference, because the most extensive comparison with observations (Zoccali & Piotto 2000), discussed below, refers to these models.

For a fixed number of MS stars, the predicted numbers of giants from different models do not completely agree. The differences at the brightest few bins are due to different BCs (c.f. Section 5.1.3), which bend the RGB by different amounts, rather than to differences in the input physics. However, even in the smooth part of the RGB LF, the models show differences as large as 0.16 dex (at $Z = 0.004$) and 0.11 dex (at $Z = 0.0001$). These imply a factor of 1.45 and 1.3 in the number counts, respectively. As discussed by Schiavon et al. (2002; see also Section 5.2.2) such discrepancies imply nonnegligible differences on integrated spectral indices. Also, the large differences among the brightest bins have a significant impact on the integrated light. For example, the Y^2 LFs predict fainter total magnitudes with respect to Girardi, even if they predict more giants all along the RGB, because they reach a fainter magnitude at the tip.

5.2.2. THE OBSERVED RGB LUMINOSITY FUNCTION It was only after the 1990s that photometry of GCs with high enough statistics on the RGB allowed the comparison between observed and theoretical LFs. From the combined LF of the metal-poor GCs NGC4590, NGC6397 and M92, Stetson (1991) found two kinds of discrepancy between the data and models: a local excess of stars just brighter than the subgiant branch and a global excess of RGB stars with respect to MS stars.

The subgiant branch excess, tentatively explained by the presence of weak interacting massive particles (Faulkner & Swenson 1993) or by deep mixing (Langer, Bolte & Sandquist 2000), was extensively investigated in M30 but has not been found in more recent studies nor in most other clusters (see Hargis, Sandquist & Bolte 2004 for a recent summary).

The second discrepancy was an excess of the global number ratio of RGB to MS stars. The slope of the RGB LF was the same in the models and in the data, but there was a zero-point offset, with the models predicting fewer giants when normalized to the MS. A similar discrepancy was found by Bergbusch & Vandenberg (1992), Bolte (1994), Degl'Innocenti, Weiss & Leone (1997), and Vandenberg, Larson & De Propriis (1998), the latter interpreting the phenomenon in terms of core rotation. No such discrepancy was found, however, by Silvestri et al. (1998), Rood et al. (1999), Zoccali & Piotto (2000), Hargis, Sandquist & Bolte (2004). Two conclusions could therefore be drawn from the literature. First, because the models do not agree on the relative number of RGB to MS stars, it is expected that different authors reach different conclusions when using different models. Comparisons should be made using several model libraries before concluding that there is some unaccounted phenomenon affecting observed RGB counts. In particular, it is not surprising that the Victoria models suggest the presence of a RGB excess more often than others, because, together with Girardi, they are the ones that predict fewer giants. The extensive analysis by Zoccali & Piotto (2000), adopting the models by Straniero, Chieffi & Limongi (1997), did not show any discrepancy between theory and observations over a large metallicity range. As shown by Zoccali & Piotto (2000, their figure 4), the models by Silvestri et al. (1998) and Cassisi & Salaris (1997) are identical to the Straniero,

Chieffi & Limongi (1997) ones shown in Figure 7. The new Teramo models predict more giants in the intermediate metallicity regime ($Z = 0.004$). Because the observed LFs of GCs of this metallicity (NGC 6652, NGC 362) did agree with the Straniero, Chieffi & Limongi (1997) models (Zoccali & Piotto 2000), we should conclude that the Teramo models produce $\sim 25\%$ too many giants at this metallicity. Second, the same set of models (i.e., the Victoria ones) reproduce some clusters well (e.g., M3; as shown in Rood et al. 1999) but not others (e.g., M5, Sandquist et al. 1996; M13, VandenBerg, *private communication*). Because the metallicity of these clusters is nearly identical, we should conclude that, in addition to the model-to-model variations, some cluster-to-cluster variation in the RGB to MS number must exist. Perhaps this is due to deep mixing, as discussed by Langer et al. (2000).

A different kind of discrepancy between models and data was found by Zoccali & Piotto (2000) and Schiavon et al. (2002), namely a flattening of the observed RGB LF above the HB, resulting in an excess of observed bright giants, for metal-rich clusters only ($[\text{Fe}/\text{H}] > -1$). A similar feature was found by Sandquist et al. (1996) in M5 ($[\text{Fe}/\text{H}] = -1.3$). It is difficult to investigate the nature (and reality) of this discrepancy, due to the lack of good quality data at high metallicities (uncontaminated, low reddening GCs) and to the uncertain BCs. However, as discussed by Schiavon et al. (2002), it would have a large impact on the integrated Lick indices. It would also have an impact on the estimates of the mean SFR from the number of stars in the upper RGB.

Finally, several investigations have been devoted to setting empirical constraints on the location of the RGB-bump (e.g., Riello et al. 2003; and references therein).

5.2.3. EVOLUTION RATE AND POPULATION OF THE UPPER RGB In spite of the differences in the predicted LF among different libraries, the average SFR in a galaxy from its formation to about 1–2 Gyr ago can be estimated within a small factor from the number of RGB and AGB stars just below the tip of the RGB (TRGB). Greggio (2002) discussed the density of stars in different evolutionary phases and, in particular, in the upper RGB + AGB. She concluded that the number of stars in this region, normalized to the total mass converted into stars over the system's history, should not differ by more than a factor of a few for quite different SFHs. A. Aparicio & C. Gallart (in preparation) also present a calibration of the integrated SFR as a function of the number of stars that populate the upper RGB + AGB for several SFH scenarios and for a number of single age and composite stellar populations. They conclude that the integrated SFR from the system's birth to $\simeq 2$ Gyr ago can be estimated within a factor of 2 from the star counts for a wide range of SFHs. However, the precise value of the conversion factor depends on the stellar evolution library used, by another factor of two. Thus, comparison of integrated SFRs for different systems should be done with estimates obtained using the same library. This is an expected consequence of the different evolution rates along the RGB discussed in Section 5.2.2.

5.3. The RGB as a Metallicity Indicator

The large metallicity and comparatively small age dependence of the RGB color justifies the use of the color distribution of stars on the RGB for retrieving their metallicity distribution (e.g., Mould, Kristian & Da Costa 1983; Armandroff et al. 1993; Grillmair et al. 1996; Harris & Harris 2002; Bellazzini et al. 2003; Zoccali et al. 2003; Tiede, Sarajedini & Barker 2004; Durrell, Harris & Pritchett 2004). The classical procedure consists of comparing a grid of empirical GC RGBs of known metallicities (Da Costa & Armandroff 1990). A more complex method was proposed by Saviane et al. (2000), based on analytic representations of the RGBs as a function of M_V , $(V - I)$ and $[Fe/H]$. Inversion of these equations (hyperbolas) allows one to obtain $[Fe/H]$ from the M_V and $(V - I)$ of each star (see Zoccali et al. 2003 for similar equations in $(V - K)$ and a discussion of possible biases due to the dependence of the RGB lifetime on metallicity). Because the dependence of the RGB color on metallicity has been empirically determined, the theoretical uncertainties of the RGB color are not of concern. However, for ages younger than $\simeq 4$ Gyr the effect of age cannot be neglected (see below). In addition, the sensitivity of the RGB color on age varies with metallicity: for relatively metal-rich populations, even the oldest isochrones show a significant color spread. Other indicators have been proposed for calibrating the slope or curvature of the RGB as a function of $[Fe/H]$ (see Ferraro et al. 1999 for a recent calibration and references; also Sarajedini 1994). These indicators, however, are only useful in the case of simple stellar populations.

The main source of uncertainty at the base of these methods is the assumption of a single old age, in the case of composite stellar populations for which information on the age distribution directly from the MS is not available. Other, less detailed indicators of the presence of an intermediate-age component, as a bright AGB, can and should be used.

We have used the Teramo isochrones, which provide a fine metallicity grid, to estimate the errors introduced on the derivation of metallicity distributions in the case of the erroneous assumption of a single old age (see also Frayn & Gilmore 2003). The results are summarized in Table 2. We have derived a relationship

TABLE 2 Effect of age on metallicity derivations from RGB colors

Age (Gyr)	$[Fe/H] = -1.79$		$[Fe/H] = -1.27$		$[Fe/H] = -0.66$	
	$\Delta(V-I)$	$[Fe/H]'$	$\Delta(V-I)$	$[Fe/H]'$	$\Delta(V-I)$	$[Fe/H]'$
10	0.02	-1.98	0.03	-1.44	0.05	-0.67
6	0.05	-2.21	0.07	-1.69	0.12	-0.80
4	0.08	-2.47	0.10	-1.90	0.17	-0.96
2	0.13	-2.90	0.15	-2.30	0.25	-1.33
1	0.17	—	0.20	-2.75	0.32	-1.76

Note: $\Delta(V-I)$ is the difference in $(V-I)$ color at $M_I = -3.0$ between an isochrone of given age and $[Fe/H]$, and a 13.5-Gyr-old isochrone of the same $[Fe/H]$. $[Fe/H]'$ is the $[Fe/H]$ that would be inferred for each isochrone if an old age was (erroneously) assumed. [*]

between $[\text{Fe}/\text{H}]$ and $(V - I)$ at $M_I = -3.0$ for 13.5 Gyr isochrones valid in the range $[\text{M}/\text{H}] = -2.27$ to -0.66 . We then measured the $(V - I)$ at $M_I = -3.0$ for isochrones in a range of age for each metallicity (heading line of Table 2) and calculated (a) the color shift, $\Delta(V - I)$, of isochrones of different ages with respect to the old isochrone of the same metallicity (columns 2, 4 and 6) and, as a consequence, (b) the metallicity $[\text{Fe}/\text{H}]'$ that would be inferred for that population using the derived relationship and (erroneously) assuming old age (columns 3, 5 and 7). Note that the color shifts start to become measurable (considering typical current photometric errors) for populations 4–6 Gyr old. For these populations, the corresponding error on the metallicity determination becomes substantial. It is over 1 dex for ages younger than 2 Gyr, in the sense that a metallicity lower than the actual one would be inferred. In general, if no corrections for age are performed, for a population with a spread in age, the derived metallicity dispersion will be a lower limit if metallicity has increased with time (e.g., Fornax: Saviane, Held & Bertelli 2000; Pont et al. 2004). It will, however, be an upper limit if the system has very little metallicity dispersion but a substantial age range (e.g., Leo I: Gallart et al. 1999a,b). Finally, as discussed by Saviane et al. (2000), a global shift of the RGB position to take into account a young mean age is not a correct way to deal with this effect, because different ages mimic different metallicity shifts.

5.4. The RGB Tip

The TRGB is the feature in the CMD that corresponds to He ignition in the degenerate cores of low-mass stars. Its luminosity depends on the He-core mass ($M_{\text{core}}^{\text{He}}$), which remains almost constant for ages larger than 2–3 Gyr, the exact value depending on Z . The TRGB M_I magnitude is only weakly sensitive to metallicity (Da Costa & Armandroff 1990; Lee, Freedman & Madore 1993; Salaris & Cassisi 1998), and therefore, it is an excellent distance indicator. Its use to determine distances for external galaxies dates back to Sandage (1971). Lee, Freedman & Madore (1993) used the Da Costa & Armandroff (1990) calibration to obtain distances for a number of Local Group galaxies which contain either RR Lyrae stars or Cepheids. They showed that the results from all distance indicators agree to within ± 0.1 mag in distance modulus. Ferrarese et al. (2000) used 10 Local Group galaxies containing Cepheids to calibrate the TRGB to a constant value, valid for metallicities up to $[\text{Fe}/\text{H}] \lesssim -1$. One possible issue when applying the TRGB method to galaxies is how much the position of the tip depends on the SFH. Barker, Sarajedini & Harris (2004) concluded that the TRGB is insensitive to the shape of the SFH except when it produces a stellar population with a significant young component, or when the average metallicity is greater than $[\text{Fe}/\text{H}] = -0.3$.

The empirical calibration of the TRGB magnitude for use as a distance indicator requires the measurement of its position for systems of known distance. There are two main sources of uncertainty in this. First, in order to include in the calibration the effects of age and metallicity, the tip has to be measured for single stellar populations for which these parameters are known, such as GCs. In these, however,

TABLE 3 TRGB calibrations

Reference	Calibration	Bands	BC	Z scale	Distance scale	N_{clus}^a
FCP83	$M_{bol} = -3.82 - 0.26 [Fe/H]$	UBVJHK	own	ZW84	$M_V^{HB} = 0.5-0.8^b$	26
DA90	$M_{bol} = -3.81 - 0.19 [Fe/H]$	VI	own ^c	ZW84	$M_V^{RR} = 0.82 + 0.17 [Fe/H]$ (LDZ90)	6
F00	$M_{bol} = -(3.79 \pm 0.15) - (0.15 \pm 0.11) [Fe/H]$	JHK	Mo98	CG97	$M_V^{ZAHB} = 0.23 ([Fe/H] + 1.5) + 0.595$ (F99)	10
Be04	$M_I = -3.629 + 0.676 [M/H] + 0.258 [M/H]^2$	I(JHK)	—	HRS ^d	^e	2

^aNumber of cluster used in the calibration.

^b $M_V^{HB} = 0.5, 0.7, 0.8$ for $[Fe/H] \leq -1.0, -1.0 \leq [Fe/H] \leq -0.8, [Fe/H] \geq -0.8$.

^c $BC_I = 0.881-0.243 (V - I)_0$.

^dMetallicity determinations include various sources for each cluster. The contribution of α elements to the global metallicity has been taken into account.

^eDistance to ω Cen: eclipsing binary data; 47 Tuc: average of various distance determinations.

Reference key: Be04, Bellazzini, Ferraro & Pancino 2001; CG97, Carretta & Gratton 1997; DA90, Da Costa & Armandroff 1990; F99, Ferraro et al. 2000; FCP83, Frogel, Cohen & Persson 1983; LDZ90, Lee, Demarque & Zinn 1990; Mo98, Montegriffo et al. 1998; ZW84, Zinn & West 1984. [*]

the number of stars near the tip is relatively small, and few of them fulfill the requirements established by Madore & Freedman (1995) for measurements with internal errors smaller than 0.1 mag (see also Raffelt 1990; Bellazzini et al. 2004). Second, the zero point of the GC distance scale is somewhat uncertain (Section 6.1). Finally, to use the observed TRGB to constrain stellar evolution models, its bolometric luminosity needs to be obtained, introducing further uncertainty.

In Table 3 the main results of a number of calibrations of the TRGB magnitude are summarized. In Figure 8, different model predictions for the bolometric magnitude (M_{bol}) of the TRGB as a function of metallicity are compared with the available empirical determinations in Table 3. There is a range of predicted values for the TRGB M_{bol} , which approximately bracket the empirical relations. However, as discussed by Salaris & Cassisi (1998) and Bellazzini et al. (2004), the empirical determinations of the TRGB luminosity must be considered a lower limit of its actual value, because of the typically small number of stars sampling the upper part of the RGB in GCs. More recent estimates from larger stellar samples tend to infer brighter M_{bol} for the TRGB. The theoretical run of M_{bol} with $[Fe/H]$ has a similar slope in all models, which is also similar to the empirical slope of Frogel, Cohen & Persson (1983). The other, more recent empirical relations tend to be shallower, although compatible within the errors given by Ferraro et al. (2000).

Because the luminosity of the TRGB is mainly a function of M_{core}^{He} , as is the HB luminosity, the differences between various models must be related to the physical

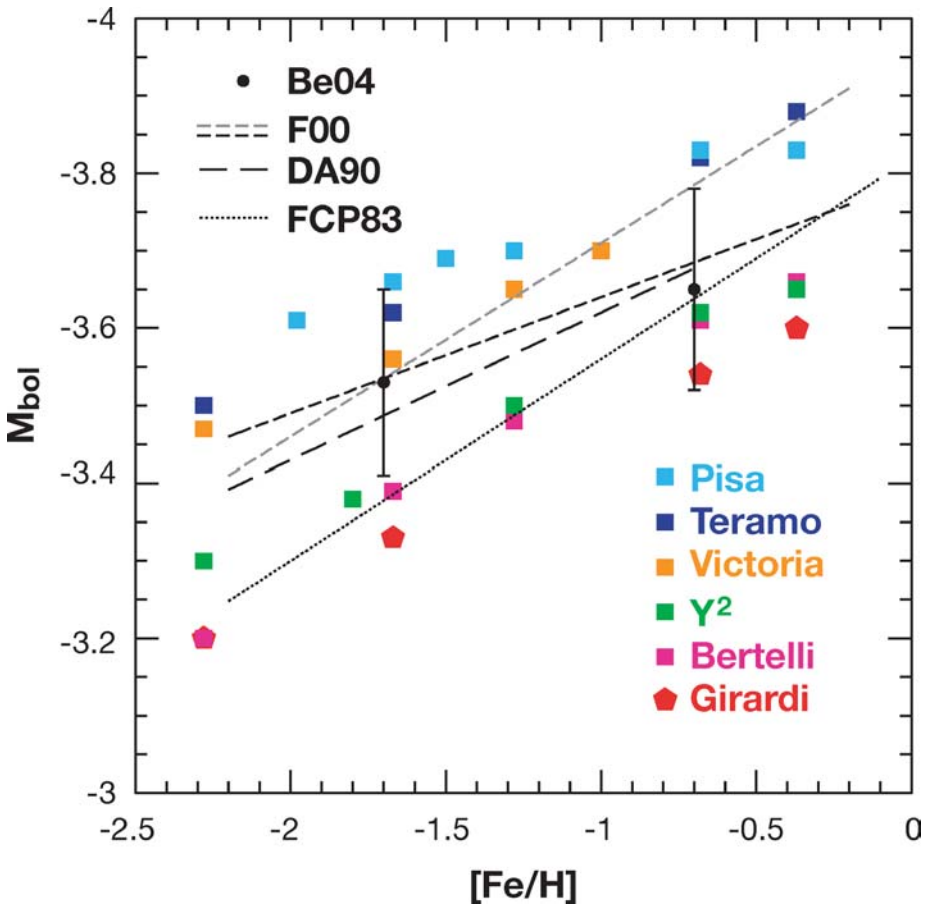


Figure 8 Comparison between the TRGB M_{bol} as predicted by current models (*color symbols*) and empirically determined by different authors (*black lines and dots*). See key for references in Table 3. BCs to transform the empirical magnitudes, in which the TRGB was measured, typically I-band values, to M_{bol} , are as provided by each author, except in the case of Be04, for which the BCs given by DA90 were used. In the case of F00, two relationships are displayed. They differ by the inclusion or not of the brightest star measured in NGC 6528 (possibly an AGB long period variable). This illustrates the kind and importance of the uncertainties inherent in the empirical determination of the TRGB. DA90 assumed the theoretical slope of the Sweigart & Gross (1978) prediction for the luminosity of the He-core flash and calculated the zero point from the data. [*]

inputs determining $M_{\text{core}}^{\text{He}}$ (Castellani et al. 2000). In fact, the ranking of TRGB luminosities follows that of HB luminosities (see Figures 8 and 9). However, as noted by Salaris et al. (2002), the Zero Age HB (ZAHB) and TRGB brightnesses have a different dependency on $M_{\text{core}}^{\text{He}}$, and therefore the consistency between the theoretical TRGB and ZAHB distance scales, checked against observational data, provides a positive indication of the models reliability (see also Caloi, D'Antona & Mazzitelli 1997; Salaris & Cassisi 1997).

6. THE CORE HE-BURNING PHASE: HORIZONTAL BRANCH, RED CLUMP, AND BLUE LOOPS

At the end of the RGB, low-mass stars ignite He in a degenerate core through the He flash and then quiescently burn it in a convective central region. Their position on the theoretical HR diagram is very narrow in luminosity, because they all have a very similar core mass, $M_c \sim 0.5 M_{\odot}$ (close to the upper limit for stability of the degenerate He core), but they may have a large extension in T_{eff} , hence the name HB. The mean HB T_{eff} depends on a number of factors, among which metallicity and the H-rich envelope mass dominate. Lower metallicity and envelope mass both produce a bluer HB. The envelope mass is determined by the initial mass of the star, but also by mass loss, mainly during the RGB and the He flash. The spread in T_{eff} typically observed along the HB of a GC of given age and metallicity is due to a spread in total mass loss. The T_{eff} dependence on envelope mass and metallicity is such that stars with masses $1 \lesssim M/M_{\odot} \lesssim M_{\text{HeF}}$, or lower mass stars in metal-rich systems, always clump on the red side of the HB, forming the so-called red clump (RC).

It has been observed that low- and intermediate-metallicity GCs with the same age and metallicity may present very different HB morphologies (Sandage & Wildey 1967, van den Bergh 1967). This implies that, in addition to age (i.e., initial mass) and metallicity, there is a so-called second parameter affecting the HB mean color, possibly by regulating the amount and variance of mass-loss during the RGB phase. Historically, some of the most popular second parameter candidates have been CO abundance (Caputo 1985; but see also Cohen & Frogel 1982), age difference³ (Bolte 1989; Lee, Demarque & Zinn 1994; Stetson et al. 1999; Catelan et al. 2001; Catelan, Ferraro & Rood, 2001; Bellazzini et al. 2001; Rey et al. 2001) although for some GCs the age hypothesis has been excluded (VandenBerg & Durrell 1990; Catelan & de Freitas Pacheco 1995; Richer et al. 1996; Catelan 1998, 2000; Sweigart & Catelan 1998), cluster concentration (Buonanno et al. 1997, Catelan et al. 2001b), deep mixing (Sweigart 1997; Cavallo & Nagar 2000), helium abundance (e.g., D'Antona & Caloi 2004) or the presence of planets (Soker & Hadar 2001). From the most recent publications it would seem

³Note that, as explained above, age certainly *is* one parameter affecting the HB morphology. The controversy is whether among galactic GCs there is an age spread large enough to explain their different HB morphologies.

that HB morphology is in fact governed by a complex interplay of several “second parameter(s).” The latest investigation (A. Recio-Blanco, A. Aparicio, G. Piotto, F. De Angeli, & S.G. Djorgovski, submitted), identifies the total luminosity of the cluster as the parameter that shows the strongest correlation with HB morphology, after metallicity.

An interesting issue is whether radial differences in HB morphology observed within some dSph galaxies (as in Sculptor: Majewski et al. 1999; Hurley-Keller, Mateo & Grebel 1999) can be interpreted as a second parameter effect. Though positive indications have been found, many of the “structural” second parameter candidates (e.g., high mass loss due to high concentration), are less likely to be effective in dSphs, and differences in HB morphology are easier to explain in terms of age and metallicity gradients (Harbeck et al. 2001).

In intermediate- and high-mass stars He burning begins in nondegenerate conditions and takes place in two different regions of the CMD. Most of the time is spent at the two color extremes of the track, at a luminosity proportional to the core mass. Therefore, the distribution of these stars in a composite CMD is concentrated in two vertical sequences: a red one near the Hayashi line (the red supergiants), and a blue one slightly redder than the MS (the blue loops).

6.1. The Horizontal Branch and Red Clump as Distance Indicators

The HB is a widely used distance indicator, because its luminosity in stellar populations older than about 8 Gyr is expected to be independent of age and only mildly dependent on metallicity. In addition, it can be measured with relatively small errors in the observed CMDs. In addition, it hosts RR Lyrae variables—relatively bright ($M_V \sim 0.65$) and easy to identify (0.2–1 day periods) pulsating stars. Unlike Cepheids, RR Lyrae do not follow a tight period-luminosity relation in optical bands (but they do in the near-IR, Longmore et al. 1990; Bono et al. 2003; Catelan, Pritzl & Smith 2004). However, as with other HB stars, their absolute mean luminosity is almost constant, hence they are prototype Population II standard candles (see Preston 1964 and Smith 1995 for reviews of their properties).

Galactic GCs are crucial for the calibration of HB stars as distance indicators. The literature of the past 20 years offers about 100 papers discussing the type and the coefficients of the relation between either $M_V(\text{RR})$ (mean magnitude of RR Lyrae, averaged over the period), $M_V(\text{HB})$ (mean magnitude of HB stars with $T_{\text{eff}} \lesssim 10000$ K), or $M_V(\text{ZAHB})$ (mean magnitude of ZAHB stars) and $[\text{Fe}/\text{H}]$. The most common result is a linear relation with slope ranging from 0.13 to 0.30 (most recently converging on 0.18; see, e.g., Carretta et al. 2000), and zero points between 0.5 and 0.9 mag. The results concerning $M_V(\text{RR})$ used to clump around a bright and a faint value, giving rise to an apparent dichotomy between short and long distance scales.

Although it is impossible to discuss these estimates in just a few pages, we show here one plot giving an idea of the current dispersion in the theoretical and

observational results. We refer the reader to the papers by Castellani, Chieffi & Pulone (1991), Caputo (1998), Fernley et al. (1998b), Chaboyer (1999), Carretta et al. (2000), VandenBerg et al. (2000), Clementini et al. (2003), Cacciari (2003), Olech et al. (2003), periodically reviewing the progress on the topic. The lower panel of Figure 9 shows the most recent theoretical relations between $M_V(\text{ZAHB})$ and $[\text{Fe}/\text{H}]$, compared with a variety of empirical data. The observations reported here are determinations of $M_V(\text{ZAHB})$ in systems whose distance is calculated by other means or directly derived from the pulsational properties of RR Lyrae. Most often, the observations give $M_V(\text{RR})$ and a conversion is applied to obtain $M_V(\text{ZAHB})$ (see below). Exceptions are the GCs in M31 (R.M. Rich, C.E. Corsi, C. Cacciari, L. Federici, F. Fusi Pecci, et al., submitted⁴), where $M_V(\text{HB})$ was measured and the conversion to $M_V(\text{ZAHB})$ was performed with the relation by Ferraro et al. (1999).

Differences in the input physics must explain at least part of the disagreement between the theoretical ZAHB locations plotted in Figure 9. In particular, models computed with the most recent input physics (the Teramo and Pisa ones) predict brighter ZAHBs, at the upper side of the empirical constraints, for reasons not yet completely understood (see Castellani et al. 2000; Cassisi et al. 2004). One parameter that is known to affect the ZAHB magnitude is the initial He content Y , with $\Delta M_V/\Delta Y = 3.64$ (Catelan et al. 1998). However, if we consider the models for $Z = 0.001$ ($[\text{Fe}/\text{H}] = -1.28$), where the differences are the largest, all the models have $Y = 0.23$ except Victoria ($Y = 0.235$), Pisa ($Y = 0.232$) and Teramo ($Y = 0.246$). Therefore, it is certainly not a $\Delta Y = 0.002$ that is the origin of the 0.27 mag difference between the Pisa and Girardi ZAHBs. Finally, different bolometric corrections and temperature-color transformations adopted by each model set may introduce additional scatter of the order of at least a few hundredths of a magnitude (Marconi et al. 2003).

Unfortunately, the empirical results do not yet allow stringent constraints on the models. The following are some reasons for the discrepancies among the data.

The most straightforward theoretical prediction is the location of the ZAHB, i.e., the beginning of the core He-burning phase. This locus is, however, very hard to identify empirically. In principle, it should coincide with the faint envelope of the magnitude distribution of HB stars. However, due to small statistics and photometric errors, in practice this is very unlikely to be the case. The most robust empirical measurement is $M_V(\text{HB})$ or $M_V(\text{RR})$. Theoretically, however, the determination of these quantities requires the construction of synthetic HBs (e.g., Ferraro et al. 1999; Demarque et al. 2000) or, in the case of $M_V(\text{RR})$, the application of the theory of pulsations (Marconi et al. 2003 showed that systematic differences up to 0.07 mag exist between the evolutionary—“static”—and pulsational approach). Recent attempts to convert between $M_V(\text{ZAHB})$ and $M_V(\text{HB})$ or $M_V(\text{RR})$ are

⁴This paper, submitted to the *Astrophysical Journal* and posted on astro-ph (0502180), revises the Fusi Pecci et al. (1996) relation for the GCs in M31. We therefore updated the relation in Figure 9.

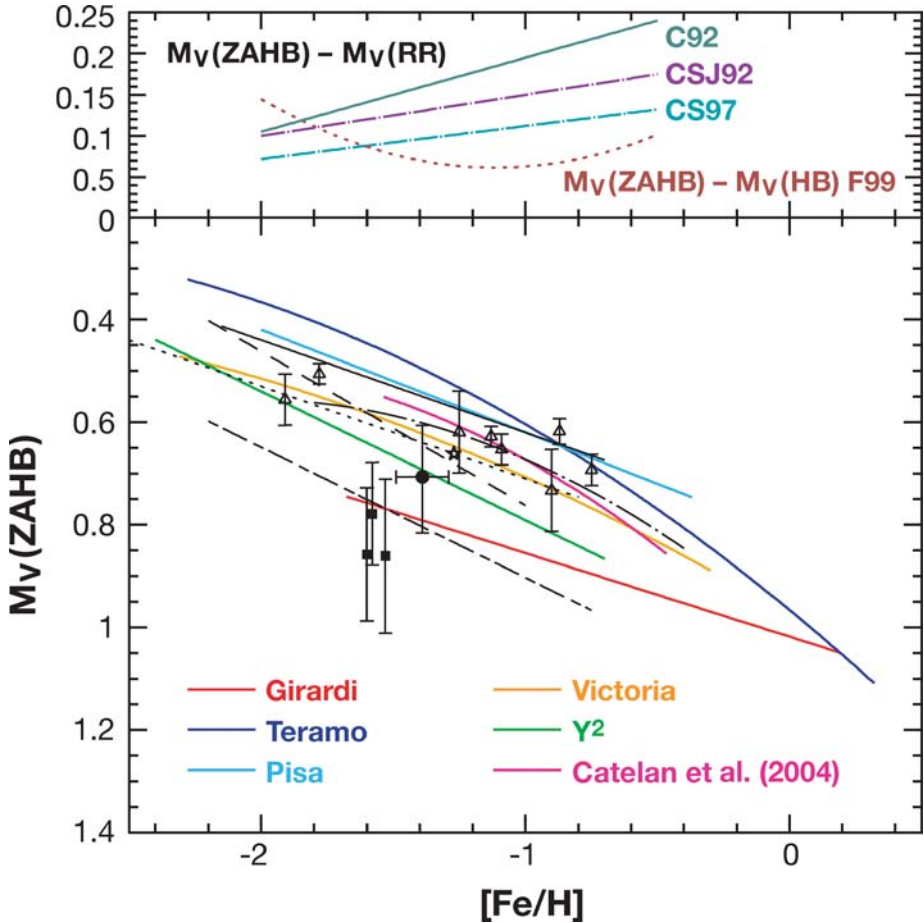


Figure 9 *Upper panel:* Relations between $M_V(RR)$ and $M_V(ZAHB)$ as determined by Catelan (1992; C92), Carney, Storm & Jones (1992; CSJ92) and Cassisi & Salaris (1997; CS97). The analogous relation between $M_V(HB)$ and $M_V(ZAHB)$ by Ferraro et al. (1999; F99) is also shown for comparison. *Lower panel:* Metallicity dependence of $M_V(ZAHB)$ from different models (*color*), compared with empirical and semi-empirical estimates (*black*): statistical parallaxes (Fernley et al. 1998b; Gould & Popowski 1998; Tsujimoto, Miyamoto & Yoshii 1998; *filled squares*), trigonometric parallaxes (Gratton 1998; *dotted line*), MS fitting (Carretta et al. 2000; *solid line*), Baade Wesselink (Clementini et al. 2003; *short-dashed-long-dashed*), RR Lyrae in ω Cen (Olech et al. 2003; *dashed line*), GCs in M31 (R.M. Rich, C.E. Corsi, C. Cacciari, L. Federici, F. Fusi Pecci, et al., submitted; *dot-dashed line*), Fourier analysis of RR Lyrae in the LMC (Alcock et al. 2004; *open star*), RR Lyrae itself (Benedict 2002; *filled circle*). Finally, the semiempirical GC ZAHBs derived by Cassisi et al. (2001) are plotted as open triangles. [*]

shown in the *upper panel* of Figure 9. All are empirical except F99. The main reason for the spread is that these are only mean equations, while the relation between $M_V(\text{RR})$ and $M_V(\text{ZAHB})$ actually depends on HB type, which in turn is governed by metallicity and the still debated second parameter(s) (Carney et al. 1992, Catelan 1992, Demarque et al. 2000). The fact that the F99 relation has a different trend is not accidental; in fact, $M_V(\text{HB})$ is different from $M_V(\text{RR})$ (Bono, Caputo & Stellingwerf 1995; Di Criscienzo, Marconi & Caputo 2004).

The empirical data in the *lower panel* of Figure 9, mostly determinations of $M_V(\text{RR})$, were converted to $M_V(\text{ZAHB})$ using the Cassisi & Salaris (1997) relation. It is an update of the relation provided by Carney et al. (1992), using only clusters with high-dispersion spectroscopic determinations of metallicity. Another likely source of scatter among empirical determinations is systematic differences between distance determinations. For example, Fernley et al. (1998a) and Groenewegen & Salaris (1999) obtain an $M_V(\text{RR})$ difference of 0.28 mag at $[\text{Fe}/\text{H}] = -1.5$ with the same sample of objects and the same $\Delta M_V/\Delta[\text{Fe}/\text{H}]$ but using statistical and reduced parallaxes, respectively. Finally, as usual when analyzing the dependence of a parameter on metallicity, we face the problems of the metallicity scale and α enhancement both deforming the x -axis of Figure 9 and, hence, the shape of the relations.

The idea of using the RC as a distance indicator is relatively old (Hatzidimitriou & Hawkins 1989, and references therein). It has recently been revived by Paczyński & Stanek (1998), who noticed that the M_I magnitude of RC stars was constant with color, both in the *HIPPARCOS* and in the Bulge OGLE CMDs. This was taken as evidence that the RC M_I magnitude was independent of metallicity and, hence, a good standard candle. However, that a complicated dependence of the RC magnitude on the stellar population composition (in age, metallicity, and age–metallicity relation) existed, at least theoretically, was demonstrated and quantified soon thereafter by Cole (1998), Girardi et al. (1999), and Girardi & Salaris (2001; see this reference for a detailed and critical historical account of the arguments given for and against the RC as a reliable distance indicator). Other authors have explored the possibility that the K magnitude of the RC might be less sensitive to population effects and reddening uncertainties, with no clear consensus (see Alves 2000; Grocholski & Sarajedini 2002; Salaris & Girardi 2002; Pietrzynski, Gieren & Udalski 2003).

6.2. The Horizontal Branch and Red Clump as Probes of Star Formation History

Given that only old populations may develop a blue HB, the presence of the latter in a galaxy is usually interpreted as clear evidence of an old component, even if its absence does not necessarily exclude old ages. However, a well populated RC traces both the old and the intermediate-age populations: the core He-burning stars with ages between $\simeq 1$ and 13 Gyr in almost the whole range of metallicity (except the oldest and most metal-poor) present in a composite stellar system are concentrated

in a very small area of the CMD. This implies that only limited information on the SFH may be inferred from the RC, especially after observational errors and theoretical uncertainties are taken into account. In addition, the age distribution in the clump is strongly biased toward relatively young (1–3 Gyr) ages and, because metallicity usually increases with time, toward the higher metallicities present in the stellar system (Girardi & Salaris 2001).

There is, however, one particular feature, the so-called secondary clump, that can provide specific information on a particular range of ages. Piatti et al. (1999) noted its presence as a faint extension of the ordinary RC in the CMDs of several LMC fields. This feature is a classic prediction of stellar evolution theory. Girardi et al. (1998) discussed thoroughly the characteristics of such a feature in the CMDs of stellar populations containing relatively metal-rich ($Z \gtrsim 0.004$), ~ 1 Gyr old stars. The theoretical predictions were refined by Girardi (1999). These two papers describe the evolutionary origin of the complex RC morphology, demonstrating that the secondary clump is made of stars with mass in a narrow range ($0.3 M_{\odot}$) above the limit for nondegenerate He ignition. It is the faint extremity of a vertical structure in the CMD, formed by core He-burning stars of increasing mass.

Figure 10 shows the RC morphology for simulated stellar populations with constant SFR(t), and single metallicity, as predicted by the Girardi and Teramo stellar evolution libraries. The general trends are common to both libraries: the mean color of the RC (and RGB) gets redder, and the RC color range gets larger as the metallicity increases. The secondary clump appears only for $Z \gtrsim 0.004$. The age differences between the two libraries are consistent with those already discussed for the MS: at around 1 Gyr, the same feature, populated by stars of similar mass, is older in the Teramo library. Also, the secondary clump of the most metal-rich population is bluer in the Teramo models, as is the oldest part of the RC, which corresponds to the HB in the low metallicity models. In fact, the differences in the overall morphology of the RC seem to be driven by a shift toward bluer colors of the old portion of the RC in the Teramo models. On another hand, the Teramo RCs are slightly brighter, as are the ZAHBs in Figure 9 (see Castellani et al. 2000 for a discussion).

As an example, Figure 10 (*right panel*) shows a fit for the LMC RC morphology (C. Gallart, P.B. Steson, F. Pont, E. Hardy & R. Zinn, in preparation) using both the Girardi and the Teramo models. A qualitative agreement is obtained with both sets, assuming the same age–metallicity relation and a constant SFR. The age–metallicity relation was constrained as follows. The metallicity of the 1 Gyr old population was set to $Z = 0.004$, with a spread of ± 0.002 , in order to reproduce the color and width of the secondary clump. A metallicity increase at younger ages is required to match the red color of the RC bright extension (which, at fixed metallicity, is bluer in the Girardi models). This example illustrates the potential use of the RC as a tracer of the age–metallicity relation in a composite stellar population in the presence of a secondary clump. The question is, of course, how well the models reproduce the data of single-age stellar populations of known age and metallicity.

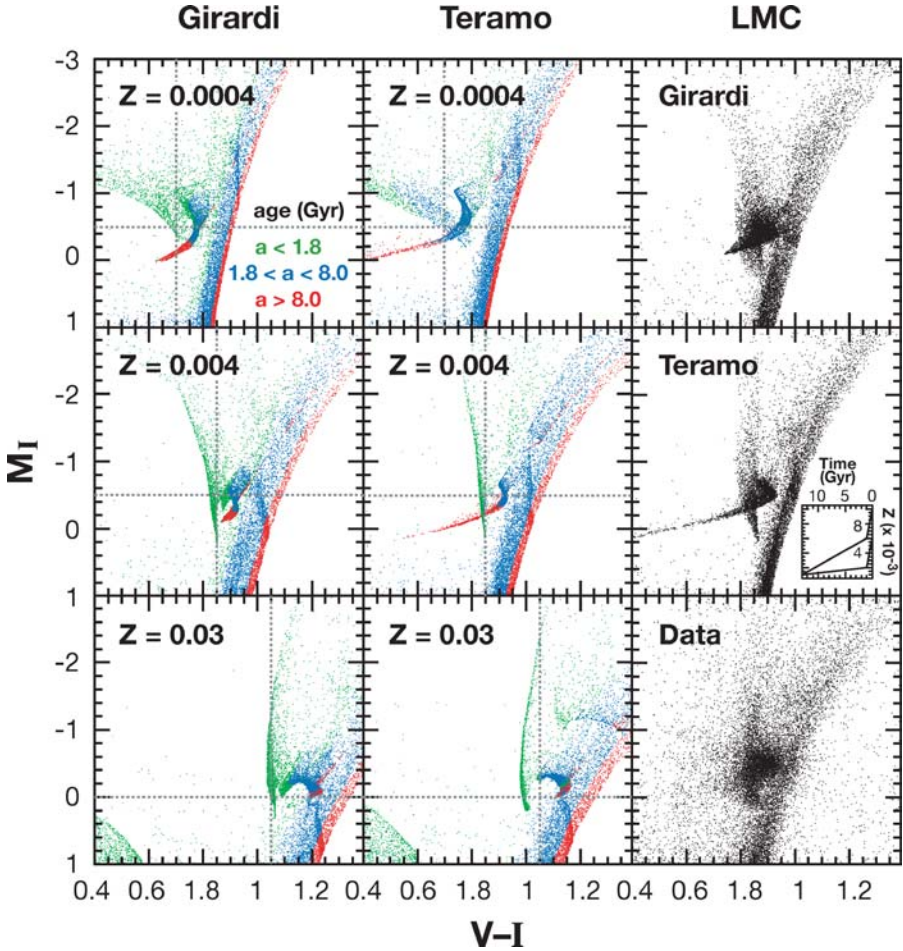


Figure 10 (Left and middle panel) RC morphology for six synthetic CMDs computed assuming a constant star formation rate, a constant metallicity, and either the Girardi or the Teramo stellar evolution models as indicated in the labels. Other features that can be noticed in the CMDs are the RGB-bump, which is clearly visible as a narrow strip of stars whose luminosity decreases for older ages and higher metallicities, and the AGB-bump, which can be noticed in the two most metal-rich models ($Z = 0.004$ and $Z = 0.03$), and more clearly in the Teramo case at $M_I \simeq -1.2$. Lines at arbitrary color and magnitude have been drawn to guide the eye in the comparison between the CMDs calculated with the two libraries. (Right panel) Simulation of the LMC RC using the two stellar evolution libraries mentioned above, with the same assumptions on the age–metallicity relation in both, with constraint as explained in the text. The age–metallicity relation is represented in the inset (stars at each age have metallicities randomly distributed between the two lines). Note that this results in a metallicity $Z = 0.004 \pm 0.002$ 1 Gyr ago. The central metallicity and its dispersion is necessary to place the secondary clump in the right color and simulate its color dispersion, respectively.

Udalski (1998) observed 15 LMC and SMC clusters and concluded that the RC M_I magnitude is constant for ages in the range of 2–10 Gyr, whereas it fades substantially (by 0.3–0.4 mag) for older stars. Sarajedini (1999) compared the RC of Galactic open clusters with internally consistent distance estimates with the Girardi models and found indications that the M_I RC magnitude does depend on age and metallicity. These data, together with that of Twarog, Anthony-Twarog & Bricker (1999) and Corsi et al. (1994), are rediscussed by Girardi (1999) and Girardi & Salaris (2001). They claim that no firm conclusion can be reached about the behavior of the mean M_I RC magnitude as a function of age and metallicity for ages greater than 2 Gyr, because of the small sample of clusters and the current uncertainties in their age and metallicities. Data for clusters younger than 2 Gyr have not been discussed so far in this context. This age range is particularly interesting because it is the one within which the secondary clump is produced. Finally, another dataset with which the theoretical predictions have been compared is the local RC as measured by *HIPPARCOS*. The advantage in this case is that the distance of each star is known. The disadvantage is that the morphology of the RC is dependent on the unknown age–metallicity relation and the range of ages present. However, with reasonable assumptions about the local SFH, Girardi et al. (1998) find a fair agreement between the observed and predicted morphologies (except for a shift in color of about $\Delta(V - I) = -0.08$, which they attribute to uncertainties in the $(V - I)$ color transformations of Kurucz 1992).

Finally, an age indicator introduced by Hatzidimitriou (1991) is the color difference between the median color of the RC and the RGB at the level of the HB. Her empirical relation has been compared by Girardi (1999) to the Girardi library. The conclusion is that the empirical trend is clearly present in the models, except maybe for the solar metallicity models, which may underestimate the color difference.

6.3. Blue Loops and Red Supergiants

Dohm-Palmer et al. (1997) have illustrated the use of blue loops as tracers of the recent SFH. They have two main advantages compared with MS stars: (a) They are $\simeq 2$ magnitudes brighter than MS stars of the same age, and (b) there is little overlap of different generations at the same magnitude, as is the case for MS stars. The main drawbacks are the smaller number of blue-loop stars and the fact that our understanding of their evolution is subject to larger uncertainties.

The most important dependences of blue-loop behavior on the adopted physical assumptions, as discussed for example by Stothers & Chin (1991), Renzini et al. (1992), Langer & Maeder (1995), Salasnich, Bressan & Chiosi (1999), Bono et al. (2000), and Maeder & Meynet (2001, and references therein), can be summarized as follows. When large overshooting is assumed at the edge of the convective cores during the MS, blue loops are dramatically reduced or suppressed. However, they can reappear if overshooting at the base of the convective envelope is also assumed. Convective core overshooting during the core He-burning phase prolongs the lifetime in this phase and increases the blue-loop T_{eff} range. Rotation and mass-loss also affect blue-loop evolution, both shortening the T_{eff} excursion. Finally they are affected by the cross-section of some nuclear reactions,

especially the $^{12}\text{C}(\alpha, \gamma)^{16}\text{O}$ reaction, whose increase has the effect of lengthening the blue loops.

The most outstanding discrepancy between observations and theory is in the ratio of blue-to-red supergiants (B/R ratio). Langer & Maeder (1995) show that, for a given luminosity range, B/R steeply increases with metallicity. Most models are able to reproduce B/R at either high or low metallicity but not self-consistently over the whole range. Most studies have measured the B/R ratio of all stars brighter than a given absolute magnitude limit and therefore integrated over a range of age. In contrast, Dohm-Palmer & Skillman (2002) have analyzed it as a function of magnitude/age in the dIrr galaxy Sextans A ($Z \simeq 0.001$). They found that the functional form of B/R as a function of age is correctly predicted by the Geneva models, although lower by a factor of two. Finally, Dohm-Palmer et al. (1997) showed that both the Bertelli and the Geneva models of the appropriate metallicity reproduced the position of the blue and red supergiants in the CMD over the entire luminosity range.

7. SUMMARY

We have compared the predictions of the current, most complete sets of stellar evolution models, both among models themselves and whenever possible with observations, to provide an estimate of their current uncertainties and their impact in the interpretation of the CMD of resolved stellar populations. With this, we hope to encourage the modelers to further improve the already excellent stellar evolution libraries and the observers to provide more stringent observational constraints. On the theoretical side, a large improvement in the accuracy and reliability of the current evolutionary scenario could be attained as a consequence of a better knowledge of (a) the actual efficiency of overshooting at the border of the convective core of intermediate-mass stars, (b) the conductive opacities and neutrino energy losses—which have a strong effect on the size of the He core at the TRGB and, in turn, control both the TRGB luminosity and the HB brightness—and (c) the correct nuclear cross-section for the $^{12}\text{C}(\alpha, \gamma)^{16}\text{O}$ reaction, which regulates the core He-burning lifetime, as well as the chemical profile of the CO cores. On the observational side, a number of new facilities will provide key data to constrain stellar evolution models. The *GAIA* satellite will provide accurate distances and physical parameters for $\simeq 10^9$ stars, whereas the *COROT* mission is specifically designed to test stellar evolution theory by providing, by means of asteroseismology, key information on stellar interiors for different types of stars through the whole HR diagram. From the ground, the *VLT* will provide accurate stellar angular diameters, which, coupled with spectral information, will allow, for example, the calibration of T_{eff} with spectral type, which is particularly needed for cold giant stars. Instruments such as *FLAMES* and *UVES* at the *VLT* are specifically designed to obtain accurate chemical abundances for a large number of stars. Finally, the many projects designed for planet or microlensing searches have, as a by-product, the discovery of large numbers of variable stars, such as eclipsing binaries, bump Cepheids and

RR Lyrae. These are useful stellar evolution probes. The importance of providing further constraints on stellar evolution models should not be underestimated, and telescope Time Allocation Committees should be persuaded to allocate the necessary resources to obtain data of the best quality for calibration and testing of stellar evolution models. These are at the basis of most aspects of astrophysics research.

In what follows, we summarize the main pros and cons of the different CMD branches for inferring the properties of a stellar system.

7.1. The Main Sequence

- Ages predicted by different models agree very well (± 0.01 Gyr) at young ages (~ 0.1 Gyr), but they may differ by up to 1 Gyr in the intermediate and old age regimes. These differences may be negligible for stellar population studies (both in percentage age and in magnitude, compared with current observational errors) at ~ 13 Gyr, but are substantial at intermediate ages. The reason for the discrepancy at intermediate ages, only part of which seems to be related to differences in the overshooting treatment, needs to be further investigated with specifically designed observations. In the meantime, it is advisable to derive SFHs with different models in order to estimate systematic errors.
- It is desirable that a larger number of stellar evolution libraries provide models calculated with different He abundances for each given metallicity, similarly to what is already done for different α enhancements.
- The trend of MS color with metallicity is a robust theoretical prediction confirmed by the latest empirical data, hence the lower MS is indeed a good indicator of the global metallicity ($[M/H]$ rather than $[Fe/H]$).
- Given the theoretical distribution of stars in the MS above the oldest MS turnoffs, the MS color function (or appropriate *à la carte* boxes) is a better SFH indicator than the most commonly used LF.

7.2. The Red Giant Branch

- The use of the RGB as a metallicity indicator is reliable when the age is known by other means and the age spread is negligible. Empirical RGB templates must be preferred, especially for $[M/H] > -0.5$, to overcome the problem of the poorly known BCs for M giants.
- Star counts on the RGB are a good indicator of the total SFR of a galaxy, from its formation to about 2–3 Gyr ago.⁵

7.3. The Horizontal Branch and Red Clump

- Neither the slope nor the zero point of the HB magnitude versus $[Fe/H]$ relation is well determined. A spread of ~ 0.3 magnitudes is present among

⁵An unknown SFH implies an uncertainty of a factor of $\simeq 2$; a similar uncertainty arises from the different predictions of the various stellar evolution model sets.

different models and among different empirical data. The use of the RC as a distance indicator is not robust because of the complex dependence of its mean absolute magnitude on the SFH of the population.

- The existence of a blue-extended HB (and/or RR Lyrae variable stars) can be considered proof of the presence of an old stellar population in a galaxy. The RC can provide important constraints on the SFH in a narrow range of ages around ~ 1 Gyr.

ACKNOWLEDGMENTS

We are very indebted to our colleague and friend Santi Cassisi for being always available (even on holidays!) to answer the theoretical questions of a desperate group of observers. We sent an advanced version of the paper to a number of colleagues and friends. They all answered quickly and with lots of suggestions that significantly improved the quality of the manuscript. Others provided occasional but not less important advice. Our thanks to: R. Carrera, M. Catelan, G. Da Costa, P. Demarque, K. Exter, L. Girardi, L. Greggio, M. Groenewegen, P. Marigo, M. Mateo, D. Minniti, N. Noël, E. Pancino, F. Pont, M. Rejkuba, A. Renzini, I. Saviane, E. Skillman, P. Stetson and D. VandenBergh. AA and CG want to acknowledge C. Chiosi, G. Bertelli and other colleagues of the Padua stellar evolution group for a fruitful, long-term collaboration. MZ and CG want to express their heartfelt thanks to M. Baffico and J.A. Rodríguez-Martín for their patience, moral support, coaching and cooking throughout the writing of this paper. J.A. also put together the whole reference list! C.G. acknowledges the hospitality of the departments of Astronomy of Princeton University, Pontificia Universidad Católica de Chile, and Osservatorio Astronomico di Teramo during the writing of this manuscript, and partial support from the Spanish Ministry of Science and Technology (Ramon y Cajal contract and grant from Plan Nacional de Investigación Científica, Desarrollo e Investigación Tecnológica, AYA2002-01939) and the European Structural Funds. MZ acknowledges the hospitality of the department of Astronomy of Princeton University. A.A. acknowledges the hospitality of the Department of Astronomy of Pontificia Universidad Católica de Chile, and partial support from the Spanish Ministry of Science and Technology (AYA 200-1661) and the European Structural Funds.

**The *Annual Review of Astronomy and Astrophysics* is online at
<http://astro.annualreviews.org>**

LITERATURE CITED

- Aerts C, Thoul A, Daszyńska J, Scuflaire R, Waelkens C, et al. 2003. *Science* 300:1926–28
- Alcock C, Alves DR, Axelrod TS, Becker AC, Bennett DP, et al. 2004. *Astron. J.* 127:334–54
- Alexander DR, Ferguson JW. 1994. *Astrophys. J.* 437:879–91

- Alonso A, Arribas S, Martínez-Roger C. 1999. *Astron. Astrophys. Suppl. Ser.* 140:261–77
- Alves DR. 2000. *Astrophys. J.* 539:732–41
- Angulo C, Arnould M, Rayet M, Descouvemont P, Baye D, et al. (NACRE Collab.) 1999. *Nucl. Phys. A* 656:3–183
- Aparicio A. 2002. See Lejeune & Fernandes 2002, p. 429–43
- Aparicio A, Gallart C. 2004. *Astron. J.* 128:1465–77
- Aparicio A, Gallart C, Bertelli G. 1997. *Astron. J.* 114:680–93
- Armandroff TE, Da Costa GS, Caldwell N, Seitzer P. 1993. *Astron. J.* 106:986–98
- Asplund M, Grevesse N, Sauval AJ. 2005. In *Cosmic Abundances as Records of Stellar Evolution and Nucleosynthesis*, ed. FN Bash, TG Barnes. ASP Conf. Ser. In press (astro-ph/0410214)
- Asplund M, Grevesse N, Sauval AJ, Prieto CA, Kiselman D. 2004. *Astron. Astrophys.* 417:751–68
- Bahcall JN, Pinsonneault MH. 1992. *Rev. Mod. Phys.* 64:885–926
- Baraffe I, Chabrier G, Allard F, Hauschildt PH. 1998. *Astron. Astrophys.* 337:403–12
- Barker MK, Sarajedini A, Harris J. 2004. *Astrophys. J.* 606:869–93
- Basu S, Antia HM. 2004. *Astrophys. J. Lett.* 606:L85–88
- Basu S, Pinsonneault MH, Bahcall JN. 2000. *Astrophys. J.* 529:1084–1100
- Behr BB, Cohen JG, McCarthy JK, Djorgovski SG. 1999. *Astrophys. J. Lett.* 517:L135–38
- Bellazzini M, Cacciari C, Federici L, Fusi Pecci F, Rich RM. 2003. *Astron. Astrophys.* 405:867–901
- Bellazzini M, Ferraro FR, Pancino E. 2001. *Astrophys. J.* 556:635–40
- Bellazzini M, Ferraro FR, Sollima A, Pancino E, Origlia L. 2004. *Astron. Astrophys.* 424:199–211
- Bellazzini M, Pecci FF, Ferraro FR, Galleti S, Catelan M, Landsman WB. 2001. *Astron. J.* 122:2569–86
- Benedict GF, McArthur BE, Fredrick LW, Harrison TE, Lee J. 2002. *Astron. J.* 123:473–84
- Bensby T, Feltzing S, Lundström I. 2004. *Astron. Astrophys.* 415:155–70
- Bergbusch PA, Vandenberg DA. 1992. *Astrophys. J. Suppl.* 81:163–220
- Bergbusch PA, Vandenberg DA. 2001. *Astrophys. J.* 556:322–39
- Bertelli G, Bressan A, Chiosi C, Fagotto F, Nasi E. 1994. *Astron. Astrophys. Suppl.* 106:275–302
- Bertelli G, Mateo M, Chiosi C, Bressan A. 1992. *Astrophys. J.* 388:400–14
- Bertelli G, Nasi E, Girardi L, Chiosi C, Zoccali M, et al. 2003. *Astron. J.* 125:770–84
- Blackwell DE, Petford AD, Arribas S, Hadcock DJ, Selby MJ. 1990. *Astron. Astrophys.* 232:396–410
- Böhm-Vitense E. 1958. *Z. Astrophys.* 46:108–43
- Bolte M. 1989. *Astron. J.* 97:1688–98
- Bolte M. 1994. *Astrophys. J.* 431:223–30
- Bono G, Caputo F, Cassisi S, Marconi M, Pierantoni L, Tornambé A. 2000. *Astrophys. J.* 543:955–71
- Bono G, Caputo F, Castellani V, Marconi M, Storm J, Degl’Innocenti S. 2003. *MNRAS* 344:1097–106
- Bono G, Caputo F, Stellingwerf RF. 1995. *Astrophys. J. Suppl.* 99:263–79
- Bono G, Castellani V, Marconi M. 2002. *Astrophys. J. Lett.* 565:L83–86
- Bressan AG, Chiosi C, Bertelli G. 1981. *Astron. Astrophys.* 102:25–30
- Brocato E, Castellani V, Di Carlo E, Raimondo G, Walker AR. 2003. *Astron. J.* 125:3111–21
- Brown TM, Ferguson HC, Smith E, Kimble RA, Sweigart AV, et al. 2003. *Astrophys. J. Lett.* 592:L17–20
- Buonanno R, Corsi C, Bellazzini M, Ferraro FR, Pecci FF. 1997. *Astron. J.* 113:706–12
- Cacciari C. 2003. In *New Horizons in Globular Cluster Astronomy*, ed. G Piotto, G Meylan, SG Djorgovski, M Riello. ASP Conf. Ser. 296:329–36
- Caloi V, D’Antona F, Mazzitelli I. 1997. *Astron. Astrophys.* 320:823–30
- Canuto VM, Mazzitelli I. 1991. *Astrophys. J.* 370:295–311
- Caputo F. 1985. *Astron. Astrophys.* 147:317–20

- Caputo F. 1998. *Astron. Astrophys. Rev.* 9:33–61
- Cariulo P, Degl’Innocenti S, Castellani V. 2004. *Astron. Astrophys.* 421:1121–30
- Carney BW, Storm J, Jones RV. 1992. *Astrophys. J.* 386:663–84
- Carretta E, Gratton RG. 1997. *Astron. Astrophys. Suppl. Ser.* 121:95–112
- Carretta E, Gratton RG, Clementini G, Pecci FF. 2000. *Astrophys. J.* 533:215–35
- Cassisi S, Castellani M, Caputo F, Castellani V. 2004. *Astron. Astrophys.* 426:641–50
- Cassisi S, Castellani V, Degl’Innocenti S, Piatto G, Salaris M. 2001. *Astron. Astrophys.* 366:578–84
- Cassisi S, Castellani V, Degl’Innocenti S, Weiss A. 1998. *Astron. Astrophys. Suppl.* 129:267–79
- Cassisi S, Salaris M. 1997. *MNRAS* 285:593–603
- Cassisi S, Salaris M, Irwin AW. 2003. *Astrophys. J.* 588:862–70
- Castellani V, Chieffi A, Pulone L. 1991. *Astrophys. J. Suppl.* 76:911–77
- Castellani V, Degl’Innocenti S. 1999. *Astron. Astrophys.* 344:97–100
- Castellani V, Degl’Innocenti S, Girardi L, Marconi M, Prada Moroni PG, Weiss A. 2000. *Astron. Astrophys.* 354:150–56
- Castellani V, Degl’Innocenti S, Marconi M, Prada Moroni PG, Sestito P. 2003. *Astron. Astrophys.* 404:645–53
- Castelli F. 1999. *Astron. Astrophys.* 346:564–85
- Castelli F, Cacciari C. 2001. *Astron. Astrophys.* 380:630–44
- Castelli F, Gratton RG, Kurucz RL. 1997. *Astron. Astrophys.* 318:841–69
- Castelli F, Kurucz RL. 2003. In *Modeling of Stellar Atmospheres*, ed. NE Piskunov, WW Weiss, DF Gray. IAU Symp. 210, pg. A20
- Catelan M. 1992. *Astron. Astrophys.* 261:443–50
- Catelan M. 2000. *Astrophys. J.* 531:826–37
- Catelan M, Bellazzini M, Landsman WB, Ferraro FR, Fusi Pecci F, Galletti S. 2001. *Astron. J.* 122:3171–82
- Catelan M, Borissova J, Sweigart AV, Spassova N. 1998. *Astrophys. J.* 494:265–84
- Catelan M, de Freitas Pacheco JA. 1995. *Astron. Astrophys.* 297:345–55
- Catelan M, Ferraro FR, Rood RT. 2001. *Astrophys. J.* 560:970–85
- Catelan M, Pritzl BJ, Smith HA. 2004. *Astrophys. J. Suppl.* 154:633–49
- Caughlan GR, Fowler WA. 1988. *Atomic Data Nucl. Data Tables* 40:283–334
- Caughlan GR, Fowler WA, Harris MJ, Zimmerman BA. 1985. *Atomic Data Nucl. Data Tables* 32:197–233
- Cavallo RM, Nagar NM. 2000. *Astron. J.* 120:1364–83
- Chaboyer B. 1999. In *Post-Hipparcos Cosmic Candles*, ed. A Heck, F Caputo, pp. 111–24. Dordrecht: Kluwer
- Chaboyer B, Fenton WH, Nelan JE, Patnaude DJ, Simon FE. 2001. *Astrophys. J.* 562:521–27
- Chaboyer B, Kim Y. 1995. *Astrophys. J.* 454:767–73
- Chaboyer B, Krauss LM. 2002. *Astrophys. J.* 567:L45–48
- Chieffi A, Straniero O, Salaris M. 1995. *Astrophys. J. Lett.* 445:L39–42
- Chiosi C, Bertelli G, Bressan A. 1992. *Annu. Rev. Astron. Astrophys.* 30:235–85
- Chiosi C, Maeder A. 1986. *Annu. Rev. Astron. Astrophys.* 24:329–75
- Christensen-Dalsgaard J, Proffitt CR, Thompson MJ. 1993. *Astrophys. J. Lett.* 403:L75–78
- Claret A. 1995. *Astron. Astrophys. Suppl.* 109:441–46
- Claret A. 2004. *Astron. Astrophys.* 424:919–25
- Claret A, Gimenez A. 1998. *Astron. Astrophys. Suppl.* 133:123–27
- Clem JL, VandenBerg DA, Grundahl F, Bell RA. 2004. *Astron. J.* 127:1127–56
- Clementini G, Gratton R, Bragaglia A, Carretta E, Di Fabrizio L, Maio M. 2003. *Astron. J.* 125:1309–29
- Clementini G, Gratton RG, Carretta E, Snedden C. 1999. *MNRAS* 302:22–36
- Coc A, Vangioni-Flam E, Descouvemont P,

- Adahchour A, Angulo C. 2004. *Astrophys. J.* 600:544–52
- Cohen JG, Frogel JA. 1982. *Astrophys. J. Lett.* 255:L39–43
- Cole AA. 1998. *Astrophys. J. Lett.* 500:L137–40
- Cordier D, Lebreton Y, Goupil MJ, Lejeune T, Beaulieu JP, Arenou F. 2002. *Astron. Astrophys.* 392:169–80
- Corsi CE, Buonanno R, Pecci FF, Ferraro FR, Testa V, Greggio L. 1994. *MNRAS* 271:385–420
- Cox JP, Giuli RT. 1968. *Principles of Stellar Structure*, Vol. II. New York: Gordon & Breach. 590 pp.
- Cox AN, Stewart JN. 1970a. *Astrophys. J. Suppl.* 19:243–59
- Cox AN, Stewart JN. 1970b. *Astrophys. J. Suppl.* 19:261–78
- Cram L. 1999. *Trans. IAU XXIIIB*, ed. J Andersen, p. 141
- Da Costa GS, Armandroff TE. 1990. *Astron. J.* 100:162–81
- D’Antona F, Caloi V. 2004. *Astrophys. J.* 611:871–80
- D’Antona F, Caloi V, Mazzitelli I. 1997. *Astrophys. J.* 477:519–34
- Degl’Innocenti S, Weiss A, Leone L. 1997. *Astron. Astrophys.* 319:487–97
- Delfosse X, Forveille T, Ségransan D, Beuzit JL, Udry S, et al. 2000. *Astron. Astrophys.* 364:217–24
- Demarque P, Zinn R, Lee YW, Yi S. 2000. *Astron. J.* 119:1398–404
- Di Criscienzo M, Marconi M, Caputo F. 2004. *Astrophys. J.* 612:1092–1106
- Dohm-Palmer RC, Skillman ED. 2002. *Astron. J.* 123:1433–37
- Dohm-Palmer RC, Skillman ED, Saha A, Tolstoy E, Mateo M, et al. 1997. *Astron. J.* 114:2527–44
- Dolphin A. 1997. *New Astron.* 2:397–409
- Dominguez I, Chieffi A, Limongi M, Straniero O. 1999. *Astrophys. J.* 524:226–41
- Dupret MA, Thoul A, Scuflaire R, Daszynska-Daszakiewicz J, Aerts C, et al. 2004. *Astron. Astrophys.* 415:251–57
- Durrell PR, Harris WE, Pritchett CJ. 2004. *Astron. J.* 128:260–70
- Elson RAW, Gilmore GF, Santiago BX. 1997. *MNRAS* 289:157–68
- Faulkner J, Swenson FJ. 1993. *Astrophys. J.* 411:200–6
- Feltzing S, Johnson RA. 2002. *Astron. Astrophys.* 385:67–86
- Fernley J, Barnes TG, Skillen I, Hawley SL, Hanley CJ, et al. 1998a. *Astron. Astrophys.* 330:515–20
- Fernley J, Carney BW, Skillen I, Cacciari C, Janes K. 1998b. *MNRAS* 293:L61–64
- Ferrarese L, Ford HC, Huchra J, Kennicutt RC, Mould JR, et al. 2000. *Astrophys. J. Suppl.* 128:431–59
- Ferraro FR, Messineo M, Pecci FF, de Palo MA, Straniero O, et al. 1999. *Astron. J.* 118:1738–58
- Ferraro FR, Montegriffo P, Origlia L, Pecci FF. 2000. *Astron. J.* 119:1282–95
- Fluks MA, Plez B, The PS, de Winter D, Westerland BE, Steenman HC. 1994. *Astron. Astrophys. Suppl.* 105:311–36
- Frayn CM, Gilmore GF. 2002. *MNRAS* 337:445–58
- Frayn CM, Gilmore GF. 2003. *MNRAS* 339:887–96
- Freedman WL, Madore BF, Gibson BK, Ferrarese L, Kelson DD, et al. 2001. *Astrophys. J.* 553:47–72
- Freytag B, Salaris M. 1999. *Astrophys. J. Lett.* 513:L49–52
- Frogel JA, Cohen JG, Persson SE. 1983. *Astrophys. J.* 275:773–89
- Fusi Pecci F, Buonanno R, Cacciari C, Corsi CE, Djorgovski SG, et al. 1996. *Astron. J.* 112:1461
- Gallagher JS, Mould JR, de Feijter E, Holtzman J, Stappers B, et al. 1996. *Astrophys. J.* 466:732–41
- Gallart C, Freedman WL, Aparicio A, Bertelli G, Chiosi C. 1999a. *Astron. J.* 118:2245–61
- Gallart C, Zoccali M, Bertelli G, Chiosi C, Demarque P, et al. 2003. *Astron. J.* 125:742–53
- Girardi L. 1999. *MNRAS* 308:818–32
- Girardi L, Bertelli G, Bressan A, Chiosi C,

- Groenewegen MAT, et al. 2002. *Astron. Astrophys.* 391:195–212
- Girardi L, Bertelli G, Bressan A, Chiosi C, Valenari A. 1999. *Baltic Astron.* 8:265–69
- Girardi L, Bressan A, Bertelli G, Chiosi C. 2000. *Astron. Astrophys. Suppl.* 141:371–83
- Girardi L, Groenewegen MAT, Weiss A, Salaris M. 1998. *MNRAS* 301:149–60
- Girardi L, Salaris M. 2001. *MNRAS* 323:109–29
- Gould A, Popowski P. 1998. *Astrophys. J.* 508:844–53
- Gratton RG. 1998. *MNRAS* 296:739–45
- Gratton RG, Bonifacio P, Bragaglia A, Carretta E, Castellani V, et al. 2001. *Astron. Astrophys.* 369:87–98
- Gratton RG, Carretta E, Desidera S, Lucatello S, Mazzei P, Barbieri M. 2003. *Astron. Astrophys.* 406:131–40
- Gratton R, Sneden C, Carretta E. 2004. *Annu. Rev. Astron. Astrophys.* 42:385–440
- Green EM, Demarque P, King CR. 1987. *The Revised Yale Isochrones and Luminosity Functions*. New Haven: Yale Obs.
- Greggio L. 2002. See Lejeune & Fernandes 2002, p. 444
- Grillmair CJ, Lauer TR, Worthey G, Faber SM, Freedman WL, et al. 1996. *Astron. J.* 112:1975–87
- Grocholski AJ, Sarajedini A. 2002. *Astron. J.* 123:1603–12
- Groenewegen MAT, Salaris M. 1999. *Astron. Astrophys.* 348:L33–36
- Haft M, Raffelt G, Weiss A. 1994. *Astrophys. J.* 425:222–30
- Harbeck D, Grebel EK, Holtzman J, Guhathakurta P, Brandner W, et al. 2001. *Astron. J.* 122:3092–105
- Hargis JR, Sandquist EL, Bolte M. 2004. *Astrophys. J.* 608:243–60
- Harris WE, Harris GLH. 2002. *Astron. J.* 123:3108–23
- Harris J, Zaritsky D. 2001. *Astrophys. J. Suppl.* 136:25–40
- Hatzidimitriou D. 1991. *MNRAS* 251:545–54
- Hatzidimitriou D, Hawkins MRS. 1989. *MNRAS* 241:667–90
- Henry TJ, McCarthy DW. 1993. *Astron. J.* 106:773–89
- Hernandez X, Valls-Gabaud D, Gilmore G. 1999. *MNRAS* 304:705–19
- Hodge P. 1989. *Annu. Rev. Astron. Astrophys.* 27:139–59
- Holtzman JA, Gallagher JS, Cole AA, Mould JR, Grillmair CJ, et al. 1999. *Astron. J.* 118:2262–79
- Holtzman JA, Mould JR, Gallagher JS, Watson AM, Grillmair CJ, et al. 1997. *Astron. J.* 113:656–68
- Hubbard WB, Lampe M. 1969. *Astrophys. J. Suppl.* 18:297–346
- Huebner WF, Merts AL, Magee NH Jr, Argo MF. 1977. *Astrophys. Opacity Libr., UC-34b*
- Hurley-Keller D, Mateo M, Grebel EK. 1999. *Astrophys. J. Lett.* 523:L25–28
- Hurley-Keller D, Mateo M, Nemeč J. 1998. *Astron. J.* 115:1840–55
- Iben I Jr. 1968. *Nature* 220:143
- Iben I Jr. 1991. *Astrophys. J. Suppl.* 76:55–114
- Iben I Jr, Renzini A. 1983. *Annu. Rev. Astron. Astrophys.* 21:271–342
- Irwin AW. 2005. <http://freeeos.sourceforge.net/>
- Itoh N, Adachi T, Nakagawa M, Kohyama Y, Munakata H. 1989. *Astrophys. J.* 39:354–64
- Itoh N, Hayashi H, Nishikawa A, Kohyama Y. 1996. *Astrophys. J. Suppl.* 102:411–24
- Itoh N, Kohyama Y. 1983. *Astrophys. J.* 275:858–66
- Itoh N, Kohyama Y, Matsumoto N, Seki M. 1993. *Astrophys. J.* 404:418
- Itoh N, Mitake S, Iyetomi H, Ichimaru S. 1983. *Astrophys. J.* 273:774–82
- Izotov YI, Thuan TX. 2004. *Astrophys. J.* 602:200–30
- Jimenez R, MacDonald J. 1996. *MNRAS* 283:721–32
- Keller SC, Wood PR. 2002. *Astrophys. J.* 578:144–50
- Kim Y, Demarque P, Yi SK, Alexander DR. 2002. *Astrophys. J. Suppl.* 143:499–511
- Kippenhahn R, Thomas HC, Weigert A. 1965. *Z. Astrophys.* 61:241–67
- Kotoneva E, Flynn C, Jimenez R. 2002. *MNRAS* 335:1147–57
- Kroupa P. 2001. *MNRAS* 322:231–46

- Kunz R, Fey M, Jaeger M, Mayer A, Hammer JW, et al. 2002. *Astrophys. J.* 567:643–50
- Kurucz RL. 1991. In *Stellar Atmospheres: Beyond Classical Models*, NATO ASI Ser. C, Vol. 341, ed. L Crivellari, I Hubeny, DG Hummer, pp. 441–48. Dordrecht: Kluwer
- Kurucz RL. 1992. In *Stellar Populations of Galaxies, IAU Symp.*, ed. B Barbuy, A Renzini, 149:225–32. Dordrecht: Kluwer
- Landre V, Prantzos N, Aguer P, Bogaert G, Lefebvre A, Thibaud JP. 1990. *Astron. Astrophys.* 240:85–92
- Langer GE, Bolte M, Sandquist E. 2000. *Astrophys. J.* 529:936–45
- Langer N, Maeder A. 1995. *Astron. Astrophys.* 295:685–92
- Lebreton Y. 2000. *Annu. Rev. Astron. Astrophys.* 38:35–77
- Lee J, Carney BW. 2002. *Astron. J.* 124:1511–27
- Lee MG, Freedman WL, Madore BF. 1993. *Astrophys. J.* 417:553–59
- Lee Y, Demarque P, Zinn R. 1990. *Astrophys. J.* 350:155–72
- Lee Y, Demarque P, Zinn R. 1994. *Astrophys. J.* 423:248–65
- Lejeune T, Cuisinier F, Buser R. 1997. *Astron. Astrophys. Suppl.* 125:229–46
- Lejeune T, Cuisinier F, Buser R. 1998. *Astron. Astrophys. Suppl.* 130:65–75
- Lejeune T, Fernandes J, eds. 2002. *Observed HR Diagrams and Stellar Evolution*, ASP Conf. Proc. Vol. 274. San Francisco: Astron. Soc. Pac.
- Lejeune T, Schaerer D. 2001. *Astron. Astrophys.* 366:538–46
- Limongi M, Straniero O, Chieffi A. 2000. *Astrophys. J. Suppl.* 129:625–64
- Longmore AJ, Dixon R, Skillen I, Jameson RF, Fernley JA. 1990. *MNRAS* 247:684–95
- Luridiana V, Peimbert A, Peimbert M, Cervio M. 2003. *Astrophys. J.* 592:846–65
- Madore BF, Freedman WL. 1995. *Astron. J.* 109:1645–52
- Maeder A, Conti PS. 1994. *Annu. Rev. Astron. Astrophys.* 32:227–75
- Maeder A, Meynet G. 1989. *Astron. Astrophys.* 210:155–73
- Maeder A, Meynet G. 2001. *Astron. Astrophys.* 373:555–71
- Majewski SR, Siegel MH, Patterson RJ, Rood RT. 1999. *Astrophys. J. Lett.* 520:L33–36
- Malkov OY. 2003. *Astron. Astrophys.* 402:1055–60
- Marconi M, Caputo F, Di Criscienzo M, Castellani M. 2003. *Astrophys. J.* 596:299–313
- Massey P. 2003. *Annu. Rev. Astron. Astrophys.* 41:15–56
- Mateo ML. 1998. *Annu. Rev. Astron. Astrophys.* 36:435–506
- McWilliam A. 1997. *Annu. Rev. Astron. Astrophys.* 35:503–56
- McWilliam A, Rich RM. 2004. In *Origin and Evolution of the Elements*, ed. A McWilliam, M Rauch. Pasadena: Carnegie Obs. Available online only at <http://www.ociw.edu/ociw/symposia/series/symposium4/proceedings.html>
- Meléndez J. 2004. *Astrophys. J.* 615:1042–47
- Mighell KJ. 1999. *Astrophys. J.* 518:380–93
- Mighell KJ, Butcher HR. 1992. *Astron. Astrophys.* 255:26–34
- Mihalas D, Hummer DG, Mihalas BW, Däppen W. 1990. *Astrophys. J.* 350:300–8
- Monaco L, Ferraro FR, Bellazzini M, Pancino E. 2002. *Astrophys. J. Lett.* 578:L47–50
- Montalbán J, D'Antona F, Mazzitelli I. 2000. *Astron. Astrophys.* 360:935–51
- Montegriffo P, Ferraro FR, Origlia L, Fusi Pecci F. 1998. *MNRAS* 297:872–84
- Mould JR, Kristian J, Da Costa GS. 1983. *Astrophys. J.* 270:471–84
- Munakata H, Kohyama Y, Itoh N. 1985. *Astrophys. J.* 296:197–203
- Ng YK, Brogt E, Chiosi C, Bertelli G. 2002. *Astron. Astrophys.* 392:1129–47
- Norris JE. 2004. *Astrophys. J. Lett.* 612:L25–28
- Olech A, Kaluzny J, Thompson IB, Schwarzenberg-Czerny A. 2003. *MNRAS* 345:86–96
- Olive KA, Steigman G, Skillman ED. 1997. *Astrophys. J.* 483:788–97
- Olsen KAG. 1999. *Astron. J.* 117:2244–67
- Olszewski EW, Suntzeff NB, Mateo M. 1996. *Annu. Rev. Astron. Astrophys.* 34:511–50

- Ortolani S, Renzini A, Gilmozzi R, Marconi G, Barbuy B, et al. 1995. *Nature* 377:701–4
- Paczynski B, Stanek KZ. 1998. *Astrophys. J. Lett.* 494:L219–22
- Palmieri R, Piotto G, Saviane I, Girardi L, Castellani V. 2002. *Astron. Astrophys.* 392:115–29
- Percival SM, Salaris M, van Wyk F, Kilkenny D. 2002. *Astrophys. J.* 573:174–83
- Piatti AE, Geisler D, Bica E, Clariá JJ, Santos JFC, et al. 1999. *Astron. J.* 118:2865–74
- Pietriferri A, Cassisi S, Salaris M, Castelli F. 2004. *Astrophys. J.* 612:168–90
- Pietrzyński G, Gieren W, Udalski A. 2003. *Astron. J.* 125:2494–501
- Pols OR, Schroder K, Hurley JR, Tout CA, Eggleton PP. 1998. *MNRAS* 298:525–36
- Pols OR, Tout CA, Eggleton PP, Han Z. 1995. *MNRAS* 274:964–74
- Pont F, Zinn R, Gallart C, Hardy E, Winnick R. 2004. *Astron. J.* 127:840–60
- Potekhin AY. 1999. *Astron. Astrophys.* 351:787–97
- Preston GW. 1964. *Annu. Rev. Astron. Astrophys.* 2:23–48
- Raffelt GG. 1990. *Astrophys. J.* 365:559–68
- Reid IN. 1999. *Annu. Rev. Astron. Astrophys.* 37:191–237
- Renzini A, Fusi Pecci F. 1988. *Annu. Rev. Astron. Astrophys.* 26:199–244
- Renzini A, Greggio L, Ritossa C, Ferrario L. 1992. *Astrophys. J.* 400:280–303
- Rey SC, Yoon SJ, Lee YW, Chaboyer B, Sarajedini A. 2001. *Astron. J.* 122:3219–30
- Ribas I, Jordi C, Gimnez. 2000. *MNRAS* 318:L55–59
- Richard O, Michaud G, Richer J, Turcotte S, Turck-Chièze S, VandenBerg DA. 2002. *Astrophys. J.* 568:979–97
- Richer HB, Harris WE, Fahlman GG, Bell RA, Bond HE, et al. 1996. *Astrophys. J.* 463:602–8
- Riello M, Cassisi S, Piotto G, Recio-Blanco A, De Angeli F, et al. 2003. *Astron. Astrophys.* 410:553–63
- Robinson FJ, Demarque P, Li LH, Sofia S, Kim YC, et al. 2004. *MNRAS* 347:1208–16
- Rogers FJ, Iglesias CA. 1992. *Astrophys. J.* 401:361–66
- Rogers FJ, Swenson FJ, Iglesias CA. 1996. *Astrophys. J.* 456:902–8
- Rood RT, Carretta E, Paltrinieri B, Ferraro FR, Fusi Pecci F, et al. 1999. *Astrophys. J.* 523:752–62
- Ross JE, Aller LH. 1976. *Science* 191:1223–29
- Rosvick JM, VandenBerg DA. 1998. *Astron. J.* 115:1516–23
- Ryan SG, Norris JE, Bessell MS. 1991. *Astron. J.* 102:303–22
- Sagar R, Subramaniam A, Richtler T, Grebel EK. 1999. *Astron. Astrophys. Suppl.* 135:391–404
- Salaris M, Cassisi S. 1997. *MNRAS* 289:406–14
- Salaris M, Cassisi S. 1998. *MNRAS* 298:166–78
- Salaris M, Cassisi S, Weiss A. 2002. *Publ. Astron. Soc. Pac.* 114:375–402
- Salaris M, Chieffi A, Straniero O. 1993. *Astrophys. J.* 414:580–600
- Salaris M, Girardi L. 2002. *MNRAS* 337:332–40
- Salaris M, Riello M, Cassisi S, Piotto G. 2004. *Astron. Astrophys.* 420:911–19
- Salasnich B, Bressan A, Chiosi C. 1999. *Astron. Astrophys.* 342:131–52
- Salasnich B, Girardi L, Weiss A, Chiosi C. 2000. *Astron. Astrophys.* 361:1023–35
- Sandage A. 1971. *Astrophys. J.* 166:13–36
- Sandage A. 1986. *Annu. Rev. Astron. Astrophys.* 24:421–58
- Sandage A, Wildey R. 1967. *Astrophys. J.* 150:469–82
- Sandquist EL, Bolte M, Stetson PB, Hesser JE. 1996. *Astrophys. J.* 470:910
- Sarajedini A. 1994. *Astron. J.* 107:618–21
- Sarajedini A. 1999. *Astron. J.* 118:2321–26
- Saviane I, Held EV, Bertelli G. 2000. *Astron. Astrophys.* 355:56–68
- Saviane I, Rosenberg A, Piotto G, Aparicio A. 2000. *Astron. Astrophys.* 355:966–78
- Schaller G, Schaerer D, Meynet G, Maeder A. 1992. *Astron. Astrophys. Suppl.* 96:269–331
- Schiavon RP, Faber SM, Rose JA, Castilho BV. 2002. *Astrophys. J.* 580:873–86
- Schroder K, Pols OR, Eggleton PP. 1997. *MNRAS* 285:696–710

- Silvestri F, Ventura P, D'Antona F, Mazzitelli I. 1998. *Astrophys. J.* 509:192–202
- Skillman ED, Gallart C. 2002. See Lejeune & Fernandes 2002, p. 535–44
- Skillman ED, Tolstoy E, Cole AA, Dolphin AE, Saha A, et al. 2003. *Astrophys. J.* 596:253–72
- Smecker-Hane TA, Cole AA, Gallagher JS, Stetson PB. 2002. *Astrophys. J.* 572:1083
- Smith HA. 1995. *RR Lyrae Stars*, ed. A King, D Lin, S Maran, J Pringle, M Ward. Cambridge: Cambridge Univ. Press. 166 pp.
- Soker N, Hadar R. 2001. *MNRAS* 324:213–17
- Stetson PB. 1991. In *The Formation and Evolution of Star Clusters*, ed. K Janes, ASP Conf. Ser., 13:88–111. San Francisco: Astron. Soc. Pac.
- Stetson PB, Bolte M, Harris WE, Hesser JE, van den Bergh S, et al. 1999. *Astron. J.* 117:247–63
- Stothers RB. 1991. *Astrophys. J.* 383:820–36
- Stothers RB, Chin C. 1991. *Astrophys. J.* 374:288–90
- Stothers RB, Chin C. 1993. *Astrophys. J.* 412:294–300
- Stothers RB, Chin C. 1995. *Astrophys. J.* 440:297–302
- Straniero O. 1988. *Astron. Astrophys. Suppl.* 76:157–84
- Straniero O, Chieffi A, Limongi M. 1997. *Astrophys. J.* 490:425–36
- Sweigart AV. 1997. *Astrophys. J. Lett.* 474:L23–26
- Sweigart AV, Catelan M. 1998. *Astrophys. J. Lett.* 501:L63–66
- Sweigart AV, Greggio L, Renzini A. 1990. *Astrophys. J.* 364:527–39
- Sweigart AV, Gross PG. 1978. *Astrophys. J. Suppl.* 36:405–37
- Thomas HC. 1967. *Z. Astrophys.* 67:420–55
- Tiede GP, Sarajedini A, Barker MK. 2004. *Astron. J.* 128:224–36
- Tolstoy E, Saha A. 1996. *Astrophys. J.* 462:672–83
- Tosi M, Greggio L, Marconi G, Focardi P. 1991. *Astron. J.* 102:951–74
- Tsujimoto T, Miyamoto M, Yoshii Y. 1998. *Astrophys. J. Lett.* 492:L79–82
- Twarog BA, Anthony-Twarog BJ, Bricker AR. 1999. *Astron. J.* 117:1816–26
- Udalski A. 1998. *Acta Astronautica* 48:383–404
- van den Bergh S. 1967. *Astron. J.* 72:70–81
- VandenBerg DA. 1992. *Astrophys. J.* 391:685–709
- VandenBerg DA, Clem JL. 2003. *Astron. J.* 126:778–802
- VandenBerg DA, Durrell PR. 1990. *Astron. J.* 99:221–28
- VandenBerg DA, Larson AM, de Propris R. 1998. *PASP* 110:98–104
- VandenBerg DA, Swenson FJ, Rogers FJ, Iglesias CA, Alexander DR. 2000. *Astrophys. J.* 532:430–52
- Venn KA, Irwin M, Shetrone MD, Tout CA, Hill V, Tolstoy E. 2004. *Astrophys. J.* 128:1177–95
- Ventura P, Zepplier A, Mazzitelli I, D'Antona F. 1998. *Astron. Astrophys.* 334:953–68
- Weaver TA, Woosley SE. 1993. *Phys. Rep.* 227:65–96
- Woo J, Demarque P. 2001. *Astron. J.* 122:1602–6
- Woo J, Gallart C, Demarque P, Yi S, Zoccali M. 2003. *Astron. J.* 125:754–69
- Wyder TK. 2001. *Astron. J.* 122:2490–523
- Yi S, Demarque P, Kim YC, Lee YW, Ree CH, et al. 2001. *Astrophys. J. Suppl.* 136:417–37
- Yi SK, Kim YC, Demarque P. 2003. *Astrophys. J. Suppl.* 144:259–61
- Zinn R, West MJ. 1984. *Astrophys. J. Suppl.* 55:45–66
- Zoccali M, Piotto G. 2000. *Astron. Astrophys.* 358:943–55
- Zoccali M, Renzini A, Ortolani S, Greggio L, Saviane I, et al. 2003. *Astron. Astrophys.* 399:931–56



CONTENTS

FRONTISPIECE, <i>Riccardo Giacconi</i>	x
AN EDUCATION IN ASTRONOMY, <i>Riccardo Giacconi</i>	1
ASTROBIOLOGY: THE STUDY OF THE LIVING UNIVERSE, <i>Christopher F. Chyba and Kevin P. Hand</i>	31
SUNGRAZING COMETS, <i>Brian G. Marsden</i>	75
THE HYDROMAGNETIC NATURE OF SOLAR CORONAL MASS EJECTIONS, <i>Mei Zhang and Boon Chye Low</i>	103
DIGITAL IMAGE RECONSTRUCTION: DEBLURRING AND DENOISING, <i>R.C. Puetter, T.R. Gosnell, and Amos Yahil</i>	139
NEW SPECTRAL TYPES L AND T, <i>J. Davy Kirkpatrick</i>	195
HIGH-VELOCITY WHITE DWARFS AND GALACTIC STRUCTURE, <i>I. Neill Reid</i>	247
STANDARD PHOTOMETRIC SYSTEMS, <i>Michael S. Bessell</i>	293
THE THREE-PHASE INTERSTELLAR MEDIUM REVISITED, <i>Donald P. Cox</i>	337
THE ADEQUACY OF STELLAR EVOLUTION MODELS FOR THE INTERPRETATION OF THE COLOR-MAGNITUDE DIAGRAMS OF RESOLVED STELLAR POPULATIONS, <i>C. Gallart, M. Zoccali, and A. Aparicio</i>	387
EVOLUTION OF ASYMPTOTIC GIANT BRANCH STARS, <i>Falk Herwig</i>	435
NEW LIGHT ON STELLAR ABUNDANCE ANALYSES: DEPARTURES FROM LTE AND HOMOGENEITY, <i>Martin Asplund</i>	481
THE DISCOVERY AND ANALYSIS OF VERY METAL-POOR STARS IN THE GALAXY, <i>Timothy C. Beers and Norbert Christlieb</i>	531
THE CLASSIFICATION OF GALAXIES: EARLY HISTORY AND ONGOING DEVELOPMENTS, <i>Allan Sandage</i>	581
MEGA-MASERS AND GALAXIES, <i>K.Y. Lo</i>	625
MOLECULAR GAS AT HIGH REDSHIFT, <i>P.M. Solomon and P.A. Vanden Bout</i>	677
DUSTY INFRARED GALAXIES: SOURCES OF THE COSMIC INFRARED BACKGROUND, <i>Guilaine Lagache, Jean-Loup Puget, and Hervé Dole</i>	727
GALACTIC WINDS, <i>Sylvain Veilleux, Gerald Cecil, and Joss Bland-Hawthorn</i>	769
DEEP EXTRAGALACTIC X-RAY SURVEYS, <i>W.N. Brandt and G. Hasinger</i>	827

DAMPED $LY\alpha$ SYSTEMS, *Arthur M. Wolfe, Eric Gawiser,
and Jason X. Prochaska* 861

INDEXES

Subject Index 919
Cumulative Index of Contributing Authors, Volumes 32–43 943
Cumulative Index of Chapter Titles, Volumes 32–43 946

ERRATA

An online log of corrections to *Annual Review of Astronomy and Astrophysics* chapters may be found at <http://astro.annualreviews.org/errata.shtml>